

# Buoyancy Effects upon Longitudinal Dispersion in Wide Well-Mixed Estuaries

R. Smith

*Phil. Trans. R. Soc. Lond. A* 1980 **296**, 467-496  
doi: 10.1098/rsta.1980.0189

## Email alerting service

Receive free email alerts when new articles cite this article - sign up in the box at the top right-hand corner of the article or click [here](#)

To subscribe to *Phil. Trans. R. Soc. Lond. A* go to: <http://rsta.royalsocietypublishing.org/subscriptions>

# BUOYANCY EFFECTS UPON LONGITUDINAL DISPERSION IN WIDE WELL-MIXED ESTUARIES

R. SMITH

*Department of Applied Mathematics and Theoretical Physics,  
University of Cambridge, Silver Street, Cambridge, U.K.*

*(Communicated by A. A. Townsend, F.R.S. – Received 3 May 1979)*

## CONTENTS

	PAGE
1. INTRODUCTION	467
2. LIST OF HYPOTHESES AND EQUATIONS	470
3. MAXIMUM-GENERALITY SCALINGS	472
4. LONG-ESTUARY APPROXIMATION	473
5. SHALLOW-WATER SCALINGS	475
6. DETAILED DESCRIPTION OF THE FLOW	476
7. FACTORIZATION OF THE DISPERSION COEFFICIENT	479
8. LOGARITHMIC VELOCITY PROFILE	481
9. DISPERSION COEFFICIENTS	485
10. A CLASSIFICATION SCHEME FOR DISPERSION MECHANISMS	489
APPENDIX	492
REFERENCES	495

As the width of a vertically well-mixed estuary increases, the longitudinal dispersion coefficient eventually reduces from a value associated with the transverse shear of the tidal current to a much smaller value associated with the oscillatory vertical shear. In this paper the final stages of this transition are investigated, with particular emphasis on buoyancy effects due to the salinity distribution. The central mathematical result relates the long-term longitudinal dispersion coefficient to the local unsteady horizontal dispersion coefficients and to the residual horizontal circulation. A useful consequence of this result is a demarcation of the parameter regimes in which the various mass-transport mechanisms are dominant. The Thames downstream of London Bridge is revealed to be buoyancy dominated.

### 1. INTRODUCTION

In recent years there have been significant advances in the understanding of the effects of flow oscillations upon the longitudinal dispersion of passive contaminants (Okubo 1967; Holley *et al.* 1970; Chatwin 1975). For vertically well-mixed estuaries with transverse diffusivity of about

$0.1 \text{ m}^2 \text{ s}^{-1}$  (Talbot & Talbot 1974) the implications depend upon whether the estuary is narrower than 100 m, wider than 500 m, or of an intermediate width. In narrow estuaries the long-term dispersion coefficient is simply an average over the tidal period of the quasi-steady dispersion coefficient associated with the transverse shear (Smith 1977). This means that initially the dispersion increases as the square of the channel breadth. For the intermediate-sized estuaries there is insufficient time between tides for significant mixing across the estuary, and the transverse shear is no longer fully effective as a dispersion mechanism. Thus, the dispersion coefficient begins to grow less rapidly with increasing estuary breadth. The maximum contribution of the transverse shear to the longitudinal dispersion coefficient occurs when the estuary breadth is about 250 m (Holley *et al.* 1970). For wide estuaries the longitudinal dispersion decreases till eventually the transverse shear is dominated by other dispersion mechanisms (Fischer 1972). In particular, the mechanism which persists out into the open sea is that associated with vertical shear (Elder 1959; Bowden 1965). The low value of the dispersion coefficient means that for wide estuaries the time-scale for longitudinal dispersion can be several months, and is well in excess of the several days necessary for lateral mixing. Thus, as is more transparently the case for narrower estuaries, for long-term dispersion the concentration gradients are principally along the estuary and it is appropriate to regard the long-term dispersion process as being primarily longitudinal.

There has been a similar advance in the understanding of buoyancy effects upon longitudinal dispersion in steady flows (Hansen & Rattray 1965; Erdogan & Chatwin 1967; Imberger 1976). The fluid in the deeper, faster moving part of the flow has originated further upstream than the more slowly moving fluid in the shallows. In this way a longitudinal density gradient leads to a transverse density gradient, and thence to a buoyancy-driven secondary flow across the channel. The secondary flow augments the transverse turbulent mixing and so tends to reduce the contaminant concentration variations across the channel. The net result is that the first noticeable effect of buoyancy is to reduce the longitudinal dispersion associated with the transverse shear in the primary flow (Smith 1976). As the longitudinal density gradient increases, the buoyancy-driven longitudinal current becomes comparable with the primary flow. At this stage the transverse shear, and hence the longitudinal dispersion coefficient, grows with increasing density gradient (Imberger 1976). Finally, when buoyancy effects are sufficiently strong, the secondary flow leads to an almost uniform contaminant concentration across the channel, and the dominant contribution to the longitudinal dispersion becomes the vertical shear in the buoyancy-driven longitudinal current (Hansen & Rattray 1965; Chatwin 1976).

Real estuaries are subjected both to tidal and to salinity effects. Thus, ideally, theoretical analyses should include at least these two effects, if only to determine for which estuarine conditions the above-cited simpler models are applicable. Fischer (1976) makes the same point in the concluding remarks to his review article on mixing and dispersion in estuaries: 'It is not yet possible to look at a given estuary, compute the values of some appropriate dimensionless parameters, and say with certainty which mass-transport mechanisms are the most important or what factors control the intrusion of salinity'.

Macqueen (1978*a*, 1979) has made a heuristic attempt to make headway with this problem. He notes that tidal and weak buoyancy effects can both be characterized as reducing the longitudinal dispersion coefficient from the reference level for a steady constant density flow. Thus, a reasonable composite model is to include two reduction factors associated separately with buoyancy and flow oscillations. For these factors Macqueen (1978*a*, 1979) uses the results

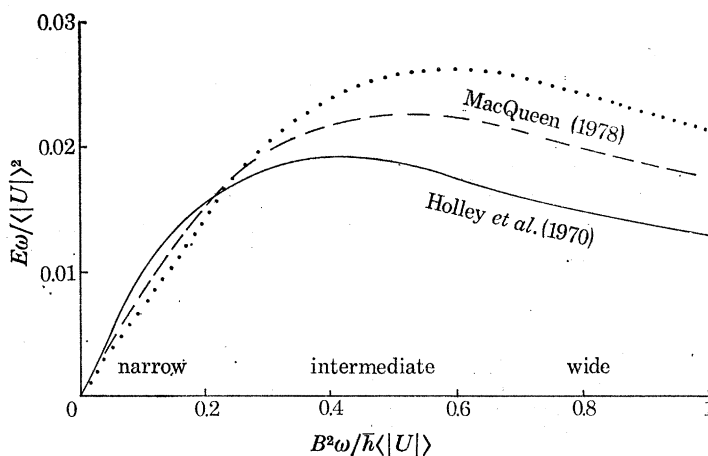


FIGURE 1. Sketch of the relationship, with and without buoyancy between the longitudinal dispersion coefficient  $E$  and the width  $2B$  in a shallow oscillatory flow, where  $\bar{h}$  is the mean depth,  $\langle |U| \rangle$  the tidally-averaged current, and  $\omega$  the angular frequency.

calculated by Smith (1976) and by Holley *et al.* (1970). An important feature of this composite modelling is that to assess the non-dimensional cross-sectional mixing time, allowance must be made for the buoyancy-driven secondary flow. The most marked effects of buoyancy are found to arise when the estuary is wide (see figure 1). The buoyancy-enhanced transverse mixing gives increased importance to the transverse shear and leads to much larger values of the longitudinal dispersion rate. Indeed, the observed longitudinal dispersion coefficient in some major estuaries, such as the Thames, can exceed the maximum values predicted by Holley *et al.* (1970). This anomaly is resolved by MacQueen's results.

The present paper is likewise directed towards the problem pointed out by Fischer (1976) in the above quotation. An analytical investigation is made of the combined effects of salinity and tides upon longitudinal dispersion in wide vertically well-mixed estuaries. As well as the oscillatory transverse and vertical shears, allowance is made for the buoyancy-driven secondary flow and longitudinal circulation. This choice of additional physical effects was motivated by Imberger's (1976) study of a non-tidal buoyancy-driven horizontal circulation, and by the need to confirm MacQueen's (1978*a*, 1979) heuristic deduction that for wide estuaries buoyancy increases the dispersion.

The analysis begins in the next section with a list of hypotheses. This unusual step for an applied mathematics paper is necessary because of the very wide range of possible mass-transport mechanisms. Nevertheless, since there are at least two modes of action for salinity and for tidal effects, the results can be expected to cover a significant range of estuarine conditions. To ensure that this is indeed the case, the subsequent derivations are based upon maximum-generality scalings. This mathematical device is exemplified in § 3, where use is made of the hypothesis that the estuary is much longer than it is wide. The following section derives the corresponding preliminary simplifications of the equations for the flow dynamics and for the contaminant dispersion. Maximum-generality scalings are used again in § 5, where this time the key hypothesis is that the estuary is much shallower than it is wide. The resulting theoretical predictions of the concentration variations across the estuary and of the flow are detailed in § 6.

One of the main fruits of this extensive analysis is arrived at in § 7. The results of § 6 are used in Fischer's (1972) formulae to obtain mathematical expressions for the three contributions to

the longitudinal dispersion associated with the steady transverse shear, the oscillatory transverse shear and the oscillatory vertical shear. For the particular class of estuaries being studied here it happens that, even with the maximum-generality scalings, the steady vertical shear gives a negligible contribution to the dispersion coefficient. An alternative derivation of these key mathematical expressions is given in the appendix.

To obtain quantitative results we need to specify the spatial structure and time-dependence of the turbulence. A particularly simple model is described in § 8. The corresponding qualitative predictions for the three contributions to the longitudinal dispersion coefficient are presented in § 9. An important aspect of these results, which is highlighted in § 10, is that they reveal the most appropriate choice of dimensionless parameters and the transition zones for the dominance of different mass-transport mechanisms. Thus, for a limited class of estuaries, we are able to answer the important question posed by Fischer (1976).

## 2. LIST OF HYPOTHESES AND EQUATIONS

It can readily be argued that salinity variations have a negligible effect upon the primary flow in a well-mixed estuary. This is because the pressure head associated with a salinity change of 32‰ is only 0.25 m, while the variation in tidal height along an estuary can be several metres (i.e. comparable with the tidal amplitude). If dispersion were simply related to the bulk flow, then no useful purpose would be served in studying the dependence of the dispersion upon the salinity gradient. However, as was first recognized by Taylor (1953), dispersion in a current is a subtle process and depends upon readily overlooked high-order aspects of the flow. In particular, it is velocity and concentration differences that are important. For example, in an extremely wide estuary, the buoyancy can cause a systematic drift whereas the tidal motion alone would periodically return a fluid element to the same position.

The above discussion serves to illustrate that, in studies of contaminant dispersion, exceptional care needs to be taken before any aspect of the flow is neglected. Equivalently, it is desirable to be precise in the specification of any simplifying assumptions. Thus, we adopt from pure mathematics the formal step of listing the hypotheses:

- (i) the estuary is much longer than the tidal excursion and the estuary width;
- (ii) the estuary is much shallower than it is wide;
- (iii) lateral mixing takes place over more than one tidal period;
- (iv) vertical mixing takes place in less than the tidal period;
- (v) longitudinal and lateral salinity gradients, vertical and lateral velocity shears all modify the dispersion;
- (vi) the turbulence can be modelled by tidal-averaged eddy diffusivity coefficients and the tidal current can be assumed to be sinusoidal in time.

The first four hypotheses exclude bay-like estuaries, steep-sided fjords, narrow estuaries, or partially stratified estuaries. However, these essentially geometrical assumptions are well satisfied by the middle and lower reaches of a major estuary such as the Thames. The fifth hypothesis ensures that we concentrate our attention upon the interesting transition regimes rather than on situations which involve only a single-dispersion mechanism. The sixth hypothesis is of an entirely technical character and is not invoked until § 8 of this paper. Its use is standard procedure in estuarine studies and greatly foreshortens the mathematical analysis. The justification for this

usage is that the horizontal dispersion coefficient can be expressed as a tidally averaged quantity (Fischer 1972), and so the detailed inter-tidal behaviour is of reduced importance.

As the underlying mathematical model for the estuary flow dynamics we represent the turbulent transports of mass and of momentum in terms of eddy-diffusivity tensors with principal axes in the longitudinal, transverse and vertical directions. The ensuing calculations reveal that the dispersion depends upon gross rather than detailed properties of the turbulence. Thus, there would be little advantage to be gained in the use of a more sophisticated higher-order turbulence closure model. Other assumptions are that we neglect channel curvature and the earth's rotation (Dyer 1978; Smith 1978*a*). Also, we make the Boussinesq approximation, and include the buoyancy effect due to salinity variations but neglect the corresponding inertia variations.

For compatibility with earlier work of the author (Smith 1976, 1977), we use a coordinate system  $(\xi, y, z, \tau)$  that moves with the cross-sectionally averaged tidal velocity  $U$ . Thus, prior to our exploiting the simplifying hypotheses (i)–(vi), the equations of motion and boundary conditions have the formidable form:

$$\partial_\tau c + (A/A_0)(u - U) \partial_\xi c + v \partial_y c + w \partial_z c = (A/A_0) \partial_\xi (\kappa_1(A/A_0) \partial_\xi c) + \partial_y (\kappa_2 \partial_y c) + \partial_z (\kappa_3 \partial_z c), \quad (2.1)$$

$$\begin{aligned} \partial_\tau u + (A/A_0)(u - U) \partial_\xi u + v \partial_y u + w \partial_z u + (A/A_0) \partial_\xi p \\ = (A/A_0) \partial_\xi (2\nu_{11}(A/A_0) \partial_\xi u) + \partial_y (\nu_{12}[\partial_y u + (A/A_0) \partial_\xi v]) + \partial_z [\nu_{13}[\partial_z u + (A/A_0) \partial_\xi w]], \end{aligned} \quad (2.2)$$

$$\begin{aligned} \partial_\tau v + (A/A_0)(u - U) \partial_\xi v + v \partial_y v + w \partial_z v + \partial_y p \\ = (A/A_0) \partial_\xi (\nu_{12}[\partial_y u + (A/A_0) \partial_\xi v]) + \partial_y (2\nu_{22} \partial_y v) + \partial_z (\nu_{23}[\partial_z v + \partial_y w]), \end{aligned} \quad (2.3)$$

$$\begin{aligned} \partial_\tau w + (A/A_0)(u - U) \partial_\xi w + v \partial_y w + w \partial_z w + \partial_z p + \beta g s \\ = (A/A_0) \partial_\xi (\nu_{13}[\partial_z u + (A/A_0) \partial_\xi w]) + \partial_y (\nu_{23}[\partial_z v + \partial_y w]) + \partial_z (2\nu_{33} \partial_z w), \end{aligned} \quad (2.4)$$

$$(A/A_0) \partial_\xi u + \partial_y v + \partial_z w = 0, \quad (2.5)$$

$$u = v = w = \partial_z c + (A/A_0)^2 \partial_\xi h \partial_\xi c + \partial_y h \partial_y c = 0 \quad \text{on} \quad z = -h, \quad (2.6)$$

$$\begin{aligned} \nu_{13}[\partial_z u + (A/A_0) \partial_\xi w] - (A/A_0) \partial_\xi \zeta [g\zeta - p + 2\nu_{11}(A/A_0) \partial_\xi u] - \partial_y \zeta \nu_{12}[\partial_y u + (A/A_0) \partial_\xi v] \\ = \nu_{23}[\partial_z v + \partial_y w] - (A/A_0) \partial_\xi \zeta \nu_{12}[\partial_y u + (A/A_0) \partial_\xi v] - \partial_y \zeta [g\zeta - p + 2\nu_{22} \partial_y v] \\ = g\zeta - p + 2\nu_{33} \partial_z w - (A/A_0) \partial_\xi \zeta \nu_{13}[\partial_z u + (A/A_0) \partial_\xi w] - \partial_y \zeta \nu_{23}[\partial_z v + \partial_y w] \\ = \partial_\tau \zeta + (A/A_0)(u - U) \partial_\xi \zeta + v \partial_y \zeta - w \\ = \partial_z c - (A/A_0)^2 \partial_\xi \zeta \partial_\xi c - \partial_y \zeta \partial_y c \\ = 0 \quad \text{on} \quad z = \zeta(\xi, y, z, \tau), \end{aligned} \quad (2.7)$$

$$\left. \begin{aligned} \nu_{ij} = \nu_{ij}(Ri), \quad \kappa_i = \kappa_i(Ri) \\ Ri = -\beta g \partial_z s / [(\partial_z u)^2 + (\partial_z v)^2]. \end{aligned} \right\} \quad (2.8)$$

with

Here  $u, v$  and  $w$  are the velocity components in the downstream transverse, and vertical directions,  $c$  the concentration of the conserved contaminant (which may be salt),  $p$  the excess pressure above the mean-hydrostatic,  $\beta g$  the reduced gravity for salt,  $\zeta$  the surface elevation,  $Ri$  the vertical gradient Richardson number,  $\kappa_i$  are eddy diffusivities for the contaminant,  $\nu_{ij}$  are eddy diffusivities for momentum, and  $A, A_0$  are the estuary cross-sectional areas at the present time and at time  $\tau = 0$ .

### 3. MAXIMUM-GENERALITY SCALINGS

Clearly, considerable simplifications will have to be made before the above equations (2.1–2.8) can be solved. The essential mathematical framework for achieving this end is as employed in the author's paper concerning buoyant contaminants in steady flows (Smith 1976). First, use is made of the geometrical fact that estuaries are typically much longer than they are wide (hypotheses (i)). A small parameter

$$\epsilon = \mathcal{B}/\mathcal{L} \quad (3.1)$$

is introduced where  $\mathcal{B}$  and  $\mathcal{L}$  are respectively representative width and length scales of the estuary (see figure 2). The governing equations (2.1)–(2.8) are to be solved only to leading order in this parameter  $\epsilon$ . This results in a separation of the equations into a longitudinal dispersion equation for the contaminant concentration, and equations in the estuary cross-sectional plane

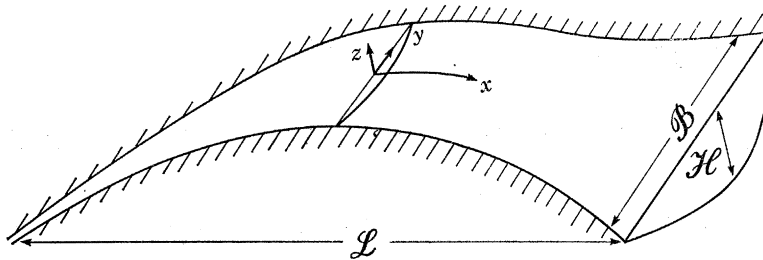


FIGURE 2. Definition sketch of length scales.

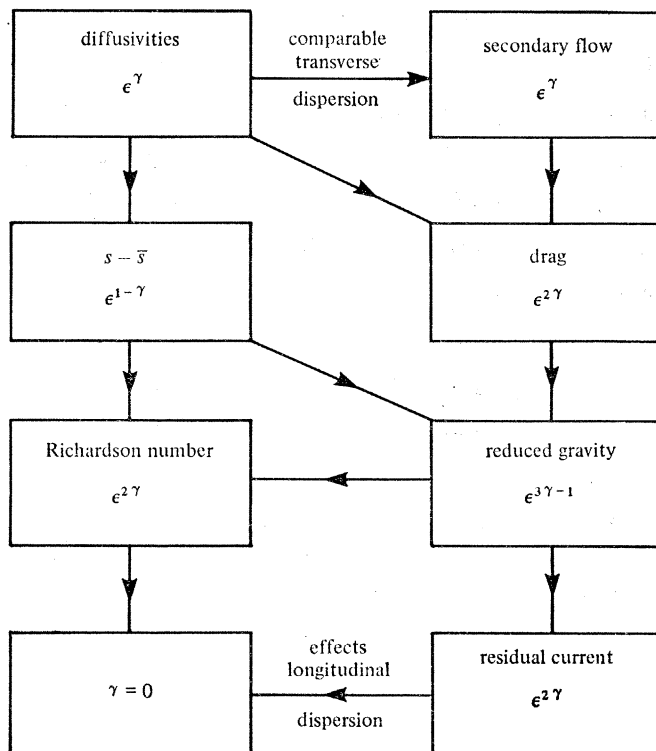


FIGURE 3. Derivation of the maximum-generality  $\epsilon$ -scalings.

for the detailed flow dynamics. The  $\epsilon$ -ordering of the many terms in the governing equations is crucial in determining which physical effects are to be retained.

Such is the wide range and large number of independent physical parameters, that appeal to the actual numerical values in one estuary might lead to a theory appropriate for just that estuary alone. Instead, we select the scalings so that certain key physical effects and as many as possible additional effects are retained. Thus, although we achieve the simplification inherent in the long estuary hypothesis (i), it is done with a minimum loss of generality. For brevity the derivation of the scalings is summarized in figure 3. The starting point is the assumption that the eddy diffusivities are of order  $\mathcal{B}\mathcal{U}\epsilon^\gamma$ , where  $\mathcal{U}$  is a typical tidal velocity and the exponent  $\gamma$  is to be determined. The final outcome is that for maximum generality the optimum choice is  $\gamma = 0$ . The full scalings, incorporating the further shallow-water hypothesis (ii), are listed in § 5.

The resulting field equations and boundary conditions, with the relative sizes of terms indicated by  $\epsilon$ -exponents, are:

$$\begin{aligned} \epsilon^2 \partial_T c + \partial_\tau c + \epsilon(1 + \epsilon A') (u - U) \partial_\xi c + v \partial_y c + w \partial_z c \\ = \partial_y (\kappa_2 \partial_y c) + \partial_z (\kappa_3 \partial_z c) + \epsilon^2 (1 + \epsilon A') \partial_\xi (\kappa_1 (1 + \epsilon A') \partial_\xi c), \end{aligned} \quad (3.2)$$

$$\partial_\tau u + v \partial_y u + w \partial_z u + \partial_\xi p = \partial_y (\nu_{12} \partial_y u) + \partial_z (\nu_{13} \partial_z u) + O(\epsilon), \quad (3.3)$$

$$\partial_\tau v + v \partial_y v + w \partial_z v + \epsilon^{-1} \partial_y p = \partial_y (2\nu_{22} \partial_y v) + \partial_z (\nu_{23} [\partial_z v + \partial_y w]) + O(\epsilon), \quad (3.4)$$

$$\partial_\tau w + v \partial_y w + w \partial_z w + \epsilon^{-1} \beta g s + \epsilon^{-1} \partial_z p = \partial_y (\nu_{23} [\partial_z v + \partial_y w]) + \partial_z (2\nu_{33} \partial_z w) + O(\epsilon), \quad (3.5)$$

$$\epsilon(1 + \epsilon A') \partial_\xi u + \partial_y v + \partial_z w = 0, \quad (3.6)$$

$$u = v = w = \partial_z c + \partial_y h \partial_y c + O(\epsilon^2) = 0 \quad \text{on} \quad z = -h, \quad (3.7)$$

$$\nu_{13} \partial_z u = \nu_{23} \partial_z v = g \zeta - p = w - \epsilon \partial_\tau \zeta = O(\epsilon^2) \quad \text{on} \quad z = \epsilon \zeta, \quad (3.8)$$

$$\nu_{ji} = \nu_{ij}(Ri), \quad \kappa_i = \kappa_i(Ri) \quad \text{with} \quad Ri = -\epsilon^{-1} \beta g \partial_z s / [(\partial_z u)^2 + (\partial_z v)^2]. \quad (3.9)$$

To revert to the original unscaled equations (2.1)–(2.8) it suffices that we ignore all the  $\epsilon$  dependence (i.e. formally set  $\epsilon = 1$ ). The major differences from the corresponding equations (1*a*–*g*) of Smith (1976) are that the tidal oscillations take place on the fast time scale  $\tau$ , rather than on the slow time scale  $T = \epsilon^2 \tau$  of the longitudinal dispersion process (Cole 1968, chap. 3), the explicit coupling between the pressure field and the tidal elevation, and the allowance for the Richardson-number dependence of the eddy diffusivities. More minor changes are that the only buoyancy effects included are those due to salinity, and the occurrence of the fractional changes

$$\epsilon A' = [A(\xi, \tau) - A_0(\xi)] / A_0(\xi)$$

in the cross-sectional area.

#### 4. LONG-ESTUARY APPROXIMATION

Proceeding as in Smith (1976) we simplify equations (3.2–3.9) by representing the dependent variables as regular power series in the small parameter  $\epsilon$ :

$$c = c^{(0)} + \epsilon c^{(1)} + \epsilon^2 c^{(2)} + \dots, \quad (4.1)$$

where  $c^{(j)}$  are independent of  $\epsilon$ . The main features are that  $c^{(0)}$  is a function only of  $(\xi, T)$ , the tidal elevation  $\zeta^{(0)}$  is uniform across the estuary, the pressure field is hydrostatic

$$p^{(0)} = g \zeta - \beta g s^{(0)} z, \quad (4.2)$$



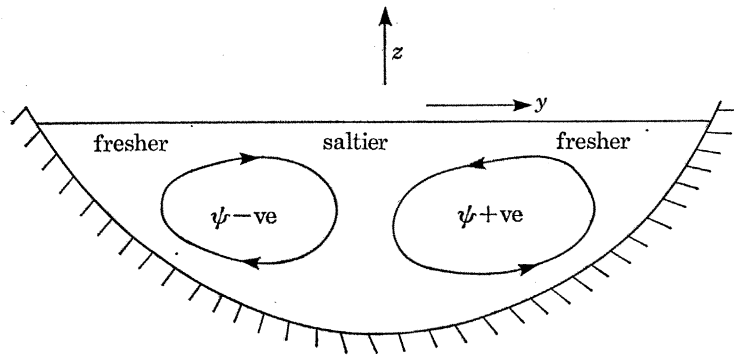


FIGURE 4. Streamlines for the secondary flow.

and that the secondary flow in the  $y-z$  plane can be described by means of a stream function (see figure 4):

$$v^{(0)} = \partial_z \psi, \quad w^{(0)} = -\partial_y \psi. \quad (4.3)$$

The detailed flow dynamics are governed by the reduced set of equations

$$\partial_\tau c^{(1)} + \partial_z \psi \partial_y c^{(1)} - \partial_y \psi \partial_z c^{(1)} - \partial_y (\kappa_2 \partial_y c^{(1)}) - \partial_z (\kappa_2 \partial_z c^{(1)}) = (U - u^{(0)}) \partial_\xi \bar{c}, \quad (4.4)$$

$$\partial_\tau u^{(0)} + \partial_z \psi \partial_y u^{(0)} - \partial_y \psi \partial_z u^{(0)} - \partial_y (\nu_{12} \partial_y u^{(0)}) - \partial_z (\nu_{13} \partial_z u^{(0)}) = -g \partial_\xi \bar{\xi} + \beta g \partial_\xi \bar{z}, \quad (4.5)$$

$$(\partial_\tau + \partial_z \psi \partial_y - \partial_y \psi \partial_z) [\partial_y^2 \psi + \partial_z^2 \psi] - (\partial_z^2 - \partial_y^2) [\nu_{23} (\partial_z^2 - \partial_y^2) \psi] - 2 \partial_y \partial_z [(\nu_{22} + \nu_{33}) \partial_y \partial_z \psi] = \beta g \partial_y s^{(1)}, \quad (4.6)$$

$$u^{(0)} = \psi = \partial_z \psi + \partial_y h \partial_y \psi = \partial_z c^{(1)} + \partial_y h \partial_y c^{(1)} = 0 \quad \text{on } z = -h, \quad (4.7)$$

$$\nu_{13} \partial_z u^{(0)} = \nu_{23} \partial_z^2 \psi = \psi = \partial_z c^{(1)} = 0 \quad \text{on } z = 0, \quad (4.8)$$

$$\nu_{ij} = \nu_{ij}(Ri^{(0)}), \quad \kappa_i = \kappa_i(Ri^{(0)}) \quad \text{with } Ri^{(0)} = -\beta g \partial_z s^{(1)} / [(\partial_z u)^2 + (\partial_z^2 \psi)^2]. \quad (4.9)$$

For clarity the superscripts  $(0)$  have been omitted on the eddy diffusivities  $\nu_{ij}^{(0)}$  and  $\kappa_i^{(0)}$ . Without loss of generality we can require that

$$U = \overline{u^{(0)}}, \quad c^{(0)} = \bar{c}, \quad \overline{c^{(1)}} = 0, \quad (4.10)$$

where the overbars denote cross-sectional average values. In particular this implies that any net flow is relegated to higher-order contributions to  $u$  (i.e. at leading order in  $\epsilon$  the bulk flow is purely oscillatory.)

The corresponding longitudinal dispersion equation can be derived by taking the cross-sectional average and then the tidal average of the order  $\epsilon^2$  terms in equation (3.2). Using angle brackets  $\langle \dots \rangle$  to denote averaging with respect to the short timescale  $\tau$ , the dispersion equation can be written

$$A_0 \partial_\tau \bar{c} + Q \partial_\xi \bar{c} - \partial_\xi (A_0 \langle (\overline{U - u^{(0)}}) c^{(1)} \rangle) - \partial_\xi (A_0 \langle \bar{\kappa}_1 \rangle \partial_\xi \bar{c}) = 0 \quad (4.11)$$

(Fischer 1972). Here  $A_0$  is the estuary cross-sectional area at  $\tau = 0$  and  $Q$  is the volume discharge rate of fresh water into the head of the estuary. Since the changes in the tidal areas and the tidal excursions are both small, it is permissible in equation (4.11) to replace  $A_0$  by any other convenient reference cross-sectional area and to replace  $\xi$  by the more usual Eulerian coordinate  $x$ .

5. SHALLOW-WATER SCALINGS

The complexity of equations (4.4)–(4.9) is evidence of the minimal loss of generality. Not only is there the full complement of buoyancy terms (Smith 1976), but also there are time derivatives admitting of the flow oscillations, and allowance for the variation in tidal height along the estuary.

Continuing as in Smith (1976), we make use of the further geometrical fact that estuaries are typically much shallower than they are wide (hypothesis (ii)). This yields a second small parameter

$$\delta = \mathcal{H} / \mathcal{B}, \tag{5.1}$$

where  $\mathcal{H}$  is a typical water depth (see figure 2). Also, we define a new vertical coordinate

$$z^* = \delta^{-1}z. \tag{5.2}$$

The effect of the  $\delta$ -expansion of the dynamical equations (4.4)–(4.9) is to decouple the lateral and vertical features of the flow field. Our aim is to achieve this simplification with a minimal loss of generality. The outcome is the scaled equations (5.5)–(5.10) given below.

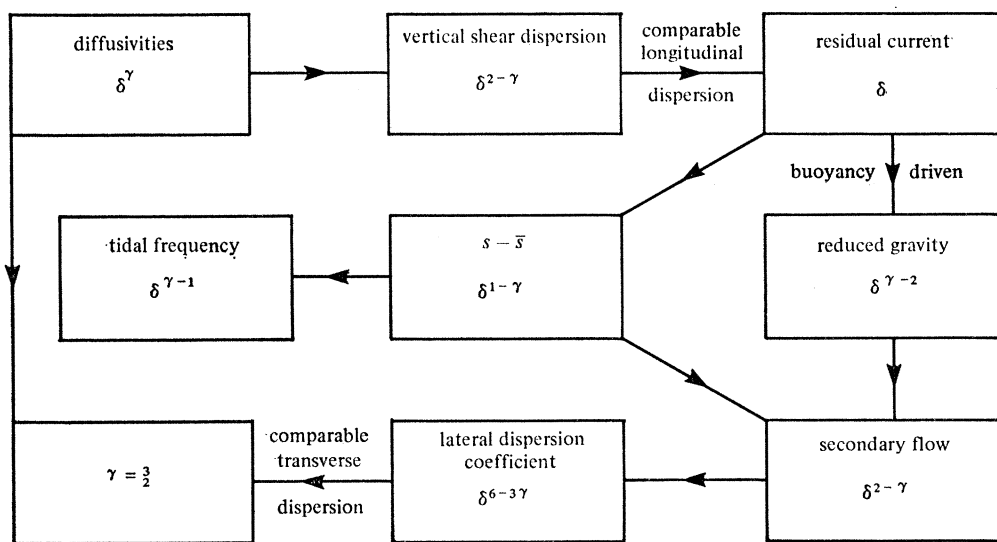


FIGURE 5. Derivation of the maximum-generality  $\delta$ -scalings.

As before, the lengthy argument leading to the maximum-generality scalings is summarized in a flow diagram (figure 5). From the initial assumption that the eddy diffusivities are of order  $\mathcal{B}\mathcal{U}\delta^\gamma$ , it eventually unfolds that to satisfy hypotheses (i)–(v) the exponent  $\gamma$  must be chosen equal to  $\frac{3}{2}$ . The analysis of §§ 3 and 4 guarantees the consistency of the  $\epsilon$ -scalings. Thus, in figure 5, only the  $\delta$ -scalings are indicated. With asterisks to denote order 1 quantities with respect to the basic dimensional scales  $\mathcal{B}$  and  $\mathcal{U}$ , the full scalings of the many physical quantities are:

$$\left. \begin{aligned} \nu_{ij} &= \delta^{\frac{3}{2}}\nu_{ij}^*, & \kappa_i &= \delta^{\frac{3}{2}}\kappa_i^*, & \zeta &= \delta^{\frac{1}{2}}\epsilon\zeta^*, \\ \psi &= \delta^{\frac{3}{2}}\psi^*, & \partial_\tau &= \delta^{\frac{1}{2}}\partial_\tau^*, & \beta g &= \delta^{\frac{1}{2}}\epsilon^{-1}\beta^*g^*, \\ g &= \delta^{-1}\epsilon^{-2}g^*, & c^{(1)} &= \delta^{-\frac{1}{2}}\epsilon c^{(1)*}, & Q &= \delta^{\frac{3}{2}}\epsilon Q^*. \end{aligned} \right\} \tag{5.3}$$

Even though the maximum-generality scalings are simply a mathematical device to ensure the retention of as many physical effects as possible, it is natural to check that their use does correspond to a physically realizable parameter régime. As a feasible specification of the basic scales we take

$$\mathcal{L} = 20 \text{ km}, \quad \mathcal{B} = 500 \text{ m}, \quad \mathcal{H} = 5 \text{ m}, \quad \mathcal{U} = 0.5 \text{ m s}^{-1} \quad \text{i.e.} \quad \epsilon = 0.025, \quad \delta = 0.01. \quad (5.4)$$

Using these scalings in the above expressions (5.9), we find that the reference values for the major physical quantities are

eddy diffusivities:	$0.25 \text{ m}^2 \text{ s}^{-1}$ ;
tidal elevation:	$1.25 \text{ m}$ ;
lateral velocities:	$0.05 \text{ m s}^{-1}$ ;
tidal frequency:	$10^{-4} \text{ s}^{-1}$ ;
reduced gravity:	$0.2 \text{ m s}^{-2}$ ;
gravity:	$80 \text{ m s}^{-2}$ ;
volume discharge rate:	$1 \text{ m}^3 \text{ s}^{-1}$ .

Most of the values indicate that the theory gives realistic weights to the corresponding physical effects. However, from the rather low estimate for the river flow rate we can deduce that in practice, the salinity distribution will tend to be pushed out towards the estuary mouth. Similarly, from the large reference value for the gravitational acceleration we can infer that, in this case, there must be a relatively large free-surface slope to maintain the tidal current, and hence that there will be significant attenuation of the tidal amplitude along the estuary.

With the asterisks and the superscripts suppressed, equations (4.4)–(4.9) can be rewritten as

$$-\partial_z(\kappa_3 \partial_z c) + \delta\{\partial_\tau c + \partial_z \psi \partial_y c - \partial_y \psi \partial_z c\} - \delta^2 \partial_y(\kappa_2 \partial_y c) = \delta(U - u) \partial_\xi \bar{c}, \quad (5.5)$$

$$-\partial_z(\nu_{13} \partial_z u) + \delta\{\partial_\tau u + \partial_z \psi \partial_y u - \partial_y \psi \partial_z u\} = -g \partial_\xi \bar{\zeta} + \delta \beta g z \partial_\xi \bar{s} + O(\delta^2), \quad (5.6)$$

$$-\partial_z^2(\nu_{23} \partial_z^2 \psi) + \delta\{\partial_\tau \psi + \partial_z \psi \partial_y \psi - \partial_y \psi \partial_z \psi\} \partial_z^2 \psi = \beta g \partial_y s + O(\delta^2) \quad (5.7)$$

$$u = \psi = \partial_z \psi + \delta^2 \partial_y h \partial_y \psi = \partial_z c + \delta^2 \partial_y h \partial_y c = 0 \quad \text{on} \quad z = -h, \quad (5.8)$$

$$\nu_{13} \partial_z u = \nu_{23} \partial_z^2 \psi = \psi = \partial_z c = 0 \quad \text{on} \quad z = 0, \quad (5.9)$$

$$\nu_{ij} = \nu_{ij}(Ri), \quad \kappa_i = \kappa_i(Ri) \quad \text{with} \quad Ri = -\beta g \partial_z s / [(\partial_z u)^2 + \delta(\partial_z^2 \psi)^2]. \quad (5.10)$$

## 6. DETAILED DESCRIPTION OF THE FLOW

To solve equations (5.5)–(5.10) we use a regular perturbation expansion in powers of  $\delta$ :

$$u = u_0 + \delta u_1 + \dots, \quad (6.1)$$

where  $u_j$  are all independent of  $\delta$ . For neatness we shall continue to suppress the  $(k)$  superscripts associated with the  $\epsilon$ -expansion. In particular,  $c$  is used to denote the small departure  $c^{(1)}$  in contaminant concentration from the cross-sectional average value  $c^{(0)} = \bar{c}$ , and there is a similar usage  $s, \bar{s}$  for the salinity.

At leading order in  $\delta$  we find that the concentration perturbation  $c_0$  is vertically uniform, that the tidal current is driven by the slope of the free surface:

$$u_0 = g \partial_\xi \bar{\zeta} \int_{-h}^z \frac{z'}{\nu_{13}} dz', \quad (6.2)$$

and that the transverse circulation is buoyancy-driven:

$$\psi_0 = \int_{-h}^z dz' \int_{-h}^z \frac{dz''}{\nu_{23}} \int_{z''}^0 \{\beta g \partial_y s_0 z''' - \tilde{\psi}'\} dz''' \quad (6.3)$$

(i.e. there is a tendency for light fluid to flow over the less dense fluid). Here  $u_0$  is required to have cross-sectional average  $U_0$ , and the integration constant  $\tilde{\psi}'$  is chosen so that the stream function is zero at the free surface.

The order  $\delta$  terms in the diffusion equation (5.5) together with the zero flux boundary conditions (5.8) and (5.9) form a non-homogeneous boundary value problem for  $c_1$ . Performing an integration with respect to  $z$  we deduce that  $c_0$  must satisfy the integrability condition

$$\partial_\tau c_0 = (U_0 - \|u_0\|) \partial_\xi \bar{c}. \quad (6.4)$$

Here we have used the notation  $\|\dots\|$  to denote the vertical average value (see table 1). Thus, the oscillatory part of the leading-order concentration perturbation is exactly out of phase with

TABLE 1. AVERAGING NOTATION

$\bar{a}$	cross-sectional average
$\langle a \rangle$	tidal time average
$a'$	fluctuating part of $a$
$\ a\ $	vertical average
$a = \langle \bar{a} \rangle + \langle \ a - \bar{a}\  \rangle + \langle a - \ a\  \rangle + \bar{a}' + \ a - \bar{a}\ ' + (a - \ a\ )'$	

the tidal current and does not contribute to the dispersion, i.e. to the first approximation there is advection back and forth along the estuary without any net dispersion.

Subject to the integrability condition (6.4) being met, the corresponding solution for the vertical concentration gradient is

$$\partial_z c_1 = \frac{\partial_\xi \bar{c}}{\kappa_3} \int_{-h}^z (u_0 - \|u_0\|) dz' + \frac{\psi_0}{\kappa_3} \partial_y c_0. \quad (6.5)$$

An immediate implication of the result (6.5) is that the Richardson number, as defined by equation (5.10), is only of order  $\delta$ . Thus, in equations (6.2), (6.3), (6.5), the eddy diffusivities should have values appropriate to constant density flows. There are a number of alternative models for the reduction in eddy diffusivities due to stratification (Breusers 1974). A model that is reasonably accurate for  $Ri < 0.25$  and particularly simple analytically is one attributed to Vreugdenhil:

$$(\nu_{13})_1 = -\frac{1}{3} (Ri)_1 (\nu_{13})_0. \quad (6.6)$$

It is only in equation (6.10) below that stratification effects need to be included. Thus, for convenience we shall omit the zero subscript and use  $\nu_{ij}$ ,  $\kappa_i$  to denote the constant density values for the eddy diffusivities.

Continuing the analysis of the diffusion equation (5.5) to order  $\delta^2$ , we obtain the further integrability condition

$$h \partial_\tau \|c_1\| = h(U_1 - \|u_1\|) \partial_\xi \bar{c} + \partial_y (h \| \kappa_2 \| \partial_y c_0) + \frac{\partial}{\partial y} \int_{-h}^0 \psi_0 \partial_z c_1 dz. \quad (6.7)$$

There is a bounded solution for  $\|c_1\|$  only if the right-hand side terms have zero tidal average (see next paragraph). Substituting from equation (6.5) for the vertical concentration gradient, and using the notation  $(\dots)'$  to denote the fluctuating part of a term, we infer that

$$h\partial_\tau \|c_1\| = h(U_1 - \|u_1\|)' \partial_\xi \bar{c} + \frac{\partial}{\partial y} \left( h\|\kappa_2 + \frac{\psi_0^2}{\kappa_3}\| \|\partial_y c_0\| \right)' + \partial_\xi \bar{c} \frac{\partial}{\partial y} \left( \int_{-h}^0 \frac{\psi_0}{\kappa_3} \int_{-h}^z (u_0 - \|u_0\|) dz_2 dz_1 \right)' \quad (6.8)$$

Since  $U_1$  is defined to be the cross-sectional average of  $u_1$ , the solution of equation (6.8) automatically satisfies the constraint  $\bar{c}'_1 = 0$  (see equation (4.10)).

The non-secularity condition invoked above yields a transverse dispersion equation for the non-oscillatory contribution to  $c_0$ . Letting  $y_+$ ,  $y_-$  denote the two sides of the estuary and performing one integration with respect to  $y$ , and also making use of the result (6.4), we obtain

$$\langle \partial_y c_0 \rangle h \langle \|\kappa_2 + \psi_0^2/\kappa_3\| \rangle = \partial_\xi \bar{c} \left\{ \int_{y_-}^{y_+} h \langle \|u_1\| \rangle dy + h \left\langle \|\kappa_2 + \psi_0^2/\kappa_3\| \int_0^\tau \partial_y \|u_0\| d\tau \right\rangle - \left\langle \int_{-h}^0 \frac{\psi_0}{\kappa_3} \int_{-h}^z (u_0 - \|u_0\|) dz_1 dz_2 \right\rangle \right\} \quad (6.9)$$

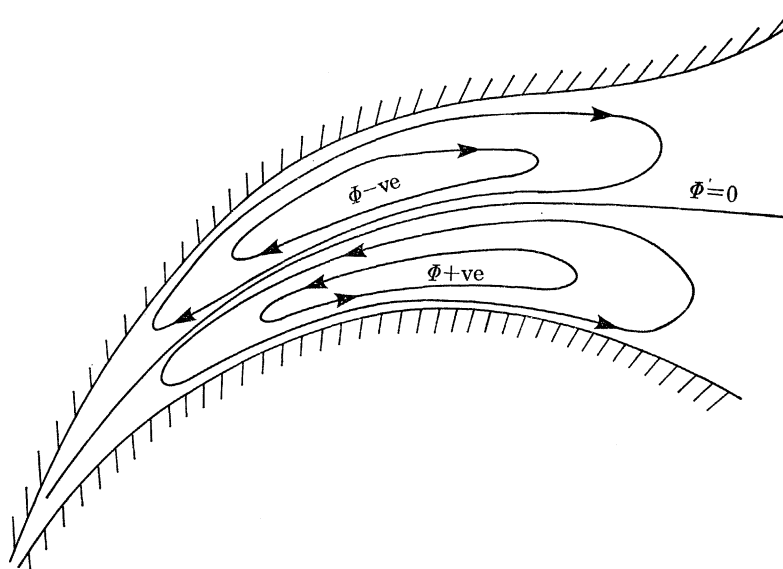


FIGURE 6. Streamlines for the residual horizontal current.

To complete our determination of the dominant terms involved in the longitudinal dispersion coefficient it remains for us to calculate the residual current  $\langle \|u_2\| \rangle$  (see figure 6). This entails solving the order  $\delta$  terms in the longitudinal momentum equation (5.6):

$$u_1 = g\partial_\xi \bar{\zeta}_1 \int_{-h}^z \frac{z_1}{\nu_{13}} dz_1 - \beta g\partial_\xi \bar{\zeta} \int_{-h}^z \frac{z_1^2}{\nu_{13}} dz_1 - g\partial_\xi \bar{\zeta}_0 \int_{-h}^z \frac{z'(\nu_{13})_1}{\nu_{13}^2} dz' - \int_{-h}^z \frac{dz_1}{\nu_{13}} \int_{z_1}^0 (\partial_\tau u_0 + \partial_z \psi_0 \partial_y u_0 - \partial_y \psi_0 \partial_z u_0) dz_2 \quad (6.10)$$

Here the residual slope  $\langle \partial_\xi \bar{\zeta}_1 \rangle$  of the free surface is determined so that the order  $\delta$  correction to the bulk velocity  $U_1 = \bar{u}_1$  is purely oscillatory.

## 7. FACTORIZATION OF THE DISPERSION COEFFICIENT

Consistent with the above  $\delta$ -expansions, the dispersion equation (4.11) becomes

$$A_0 \partial_T \bar{c} + Q \partial_\xi \bar{c} - \partial_\xi (A_0 E \partial_\xi \bar{c}) = 0, \quad (7.1)$$

with

$$E \partial_\xi \bar{c} = \langle (\overline{U_0 - u_0}) c_1 \rangle + \langle (\overline{U_1 - u_1}) c_0 \rangle. \quad (7.2)$$

It is noteworthy that in the expression (7.2) for the longitudinal dispersion coefficient  $E$ , neither of the terms

$$\langle (\overline{U_0 - u_0}) c_0 \rangle, \quad \langle \overline{\kappa_1} \rangle \partial_\xi \bar{c} \quad (7.3)$$

is retained. The first of these is identically zero owing to the exactly orthogonal phases of  $(U_0 - u_0)$  and  $c_0$ , while the turbulence term is order  $\delta$  smaller than the retained terms. This is in complete contrast to the situation for steady flows where the terms (7.3) are dominant (Smith 1976).

A nice feature of the double averaging involved in the definition (7.2) is that a decomposition of the velocity and concentration fields into steady/fluctuating and vertically uniform/vertically varying parts:

$$c_0 = \langle \|c_0\| \rangle + \langle c - \|c_0\| \rangle + \|c_0\|' + (c_0 - \|c_0\|)' \quad (7.4)$$

(see table 1) leads to a similar decomposition of the dispersion coefficient (Fischer 1972):

$$E = E_S + E_T + E_V, \quad (7.5)$$

with

$$E_S \partial_\xi \bar{c} = - \langle \|u_1\| \rangle \langle \|c_0\| \rangle, \quad (7.6)$$

$$E_T \partial_\xi \bar{c} = \langle (\overline{U_0 - \|u_0\|})' \|c_1\|' \rangle + \langle (\overline{U_1 - \|u_1\|})' \|c_0\|' \rangle, \quad (7.7)$$

$$E_V \partial_\xi \bar{c} = \langle (\overline{\|u_0\| - u_0})' (c_1 - \|c_1\|)' \rangle. \quad (7.8)$$

Here the three contributions to  $E$  are related to the steady residual circulation in the horizontal plane, the transverse oscillatory shear, and the vertical oscillatory shear. A fourth contribution, related to the steady residual circulation in a longitudinal vertical plane, does not arise until the next order in  $\delta$  (i.e. products involving  $\langle u_1 - \|u_1\| \rangle$  and  $\langle c_1 - \|c_1\| \rangle$ ). This is quite different from partially stratified estuaries, for which the above three terms are commonly neglected and only the fourth term is retained (Hansen & Rattray 1965; Chatwin 1976).

The principal shortcoming of equations (7.5)–(7.8) as regards the prediction of the salinity and other contaminant distributions along estuaries, is that the equations involve the concentration variations across the estuary. However, in the present context we have the theoretical results (6.4), (6.5), (6.8), (6.9), to provide us with that information. As a consequence of our use of maximum-generality scalings, the resulting expressions are extremely lengthy. Thus, as a preliminary we introduce the combinations of terms

$$D_0 = \left\| \frac{1}{\kappa_3} \left[ \int_{-h}^z (u_0 - \|u_0\|) dz_1 \right]^2 \right\|, \quad (7.9)$$

$$D_1 = \left\| \frac{\psi_0}{\kappa_3} \int_{-h}^z (u_0 - \|u_0\|) dz_1 \right\|, \quad (7.10)$$

$$K = \|\kappa_2 + \psi_0^2 / \kappa_3\|, \quad (7.11)$$

$$\Phi = \int_{y^-}^{y^+} h \|u_1\| dy_1, \quad (7.12)$$

$$q = \int_0^\tau \partial_y \|u_0\| d\tau, \quad (7.13)$$

Here  $D_0$ ,  $D_1$  and  $K$  have the dimensions of diffusivities and can be interpreted as being the coefficients in the local dispersion matrix for combined longitudinal and transverse dispersion (see appendix A),  $\Phi$  is a stream function for the residual horizontal circulation, and  $q$  is a dimensionless measure of the oscillatory transverse shear.

In terms of these quantities, equation (6.9) for the quasi-steady transverse concentration gradient can be re-written  $\langle \partial_y c \rangle h \langle K \rangle = \partial_y \bar{c} \{ \langle \Phi \rangle + h \langle Kq \rangle - h \langle D_1 \rangle \}$ . (7.14)

The corresponding representations for the three dominant contributions to the longitudinal dispersion coefficient are

$$E_S = \frac{1}{A_0} \int_{y^-}^{y^+} \frac{\langle \Phi \rangle^2}{h \langle K \rangle} dy, \quad (7.15)$$

$$E_T = \frac{1}{A_0} \int_{y^-}^{y^+} \left\{ h \langle Kq^2 \rangle - \frac{h \langle Kq \rangle^2}{\langle K \rangle} - h \langle D_1 q \rangle + \frac{h \langle Kq \rangle \langle D_1 \rangle}{\langle K \rangle} \right\} dy, \quad (7.16)$$

$$E_V = \frac{1}{A_0} \int_{y^-}^{y^+} \left\{ h \langle D_0 \rangle - \frac{h \langle D_1 \rangle^2}{\langle K \rangle} - h \langle D_1 q \rangle + \frac{h \langle Kq \rangle \langle D_1 \rangle}{\langle K \rangle} \right\} dy. \quad (7.17)$$

Since it is only the sum  $E_S + E_T + E_V$  that is of physical significance, the above formulae (7.15)–(7.17) have been simplified by the deletion of cancelling terms (i.e. of terms linear in  $\Phi$ ).

The leading terms in the expressions for  $E_S$ ,  $E_T$  and  $E_V$  respectively can be recognized as being in agreement with the results of Imberger (1976), Okubo (1967) and Bowden (1965). The many additional terms represent the interplay between different physical effects. Macqueen's (1978*a*) work can be regarded as being a multiplicative interpolation formula for  $E_T$  between the two limiting cases when buoyancy is dominant and when flow oscillations are dominant. The complexity of equation (7.16) would suggest that in general  $E_T$  is not separable into two factors associated with these two key physical effects (see equation (9.10) later in this paper). Such is the importance of the formulae (7.15)–(7.17) that it is desirable to check the validity of more than just the leading terms. This is done in the appendix.

Intuitively we can expect that, allowing for advection with the freshwater discharge, the tidally averaged flux of a contaminant will be directed towards regions of relatively low concentrations, i.e. that the longitudinal dispersion coefficient  $E$  is positive. At first sight the negative and cross-product terms in equations (7.16) and (7.17) would appear to admit of the opposite, unacceptable, possibility that  $E$  could be negative. Indeed, the author's original motivation for seeking an alternative derivation of these crucial formulae was the strong suspicion that for this reason they were in error. However, if we revert to the definitions (7.9)–(7.11) of the local instantaneous dispersion coefficients  $D_0$ ,  $D_1$ ,  $K$ , then it can be verified that  $E$  is given by the positive definite expression

$$E = \frac{1}{A_0} \int_{y^-}^{y^+} \left\{ \frac{\langle \Phi \rangle^2}{h \langle K \rangle} + \left\langle h \| \kappa_2 \| \left( \frac{\langle Kq \rangle - \langle D_1 \rangle}{\langle K \rangle} - q \right)^2 \right\rangle \right\} dy + \frac{1}{A_0} \int_{y^-}^{y^+} \int_{-h}^0 \left\langle \frac{1}{\kappa_3} \left( \frac{\langle Kq \rangle - \langle D_1 \rangle}{\langle K \rangle} \psi - q\psi + \int_{-h}^z (u_0 - \|u_0\|) dz_1 \right)^2 \right\rangle dz dy. \quad (7.18)$$

Thus, as befits a diffusivity, the longitudinal dispersion coefficient  $E$  is necessarily positive.

## 8. LOGARITHMIC VELOCITY PROFILE

The results of the previous section show that to evaluate the three contributions to the longitudinal dispersion coefficient it suffices that we can calculate the eddy diffusivities  $\kappa_3$ ,  $\kappa_2$  and the flow quantities  $u_0$ ,  $\psi$  and  $\langle \|u_1\| \rangle$  (i.e. the tidal current, secondary flow and the residual circulation). In general these are substantial problems in their own rights (Maxey 1978; Le Blond 1978). However, if we are satisfied with qualitative results, such as a classification scheme for wide well-mixed estuaries, then we can alleviate these difficulties by invoking hypothesis (vi). That is, the tidal oscillations are taken to be sinusoidal in time and the turbulence is modelled by tidal-averaged eddy diffusivity coefficients.

Shear dispersion depends upon the combination of velocity shear and of concentration gradients. In the wall region the eddy diffusivities  $\nu_{13}$ ,  $\nu_{23}$ ,  $\kappa_3$  for the vertical transport of momentum and of concentration become small. Thus, the velocity shear and the concentration gradient can both be large, thereby giving a significant contribution to the horizontal shear dispersion. If the channel bed is sufficiently smooth, there is in addition a thin viscous sublayer in which the eddy diffusivities approach their extremely small molecular values. The no-flux boundary condition implies that the concentration gradient tends to zero at the bed. Thus, although there can be strong velocity shears in the viscous sublayer, there is a negligible contribution to the horizontal shear dispersion. Consequently, it is principally in the turbulent wall region that the modelling of the eddy diffusivities need to be accurate and, except for small-scale laboratory experiments (Chatwin 1971, 1973), it is justifiable to ignore any viscous sub-layer. A convenient and suitably realistic model for the eddy diffusivities is

$$\nu_{13} = \hat{\nu}_{13} h \langle u_*^2 \rangle^{\frac{1}{2}} (1 - \eta) \eta, \quad \text{where} \quad \eta = \eta_* + (1 + z/h) (1 - \eta_*), \quad (8.1)$$

with similar formulae for  $\nu_{23}$  and  $\kappa_3$ . Here  $\hat{\nu}_{13}$  is a dimensionless constant (approximately 0.4),  $\langle u_*^2 \rangle^{\frac{1}{2}}$  is the root-mean square friction velocity, and  $\eta_* h$  is a roughness height. The free-surface and bottom boundary conditions are to be applied at the positions  $\eta = 1$  and  $\eta = \eta_*$ . To achieve algebraic simplifications we shall neglect explicit powers of  $\eta_*$  (i.e. roughness heights are typically only a few centimetres while water depths are several metres).

As is well known, the diffusivity distribution (8.1) leads to a logarithmic velocity profile

$$u_0 = - (gh \bar{\zeta}_0 / \hat{\nu}_{13} \langle u_*^2 \rangle^{\frac{1}{2}}) \ln (\eta / \eta_*). \quad (8.2)$$

Except near the turn of the tide, the longitudinal velocity is of order  $\delta^{\frac{1}{2}}$  greater than the transverse velocity. Thus, to a first approximation, we can take the instantaneous value of the friction velocity to be given by the formula

$$u_*^2 = |gh \bar{\zeta}_0|. \quad (8.3)$$

In particular,  $u_*$  varies as the half-power of the local water depth. Using this spatial dependence of  $\langle u_*^2 \rangle^{\frac{1}{2}}$ , it is easy to show that the free-surface slope is given by the Chezy formula

$$U_0 \langle |U_0| \rangle = - \Gamma^2 g \bar{h} \bar{\zeta}_0, \quad (8.4)$$

and that  $u_0$  is related to its cross-sectional average value  $U_0$ :

$$u_0 = U_0 (1 / \Gamma \hat{\nu}_{13}) (h / \bar{h})^{\frac{1}{2}} \ln (\eta / \eta_*). \quad (8.5)$$



Here the non-dimensional Chezy coefficient  $\Gamma$  is related to the depth profile across the estuary

$$\Gamma = \frac{1}{y_+ - y_-} \int_{y_-}^{y_+} \frac{(h/\bar{h})^{\frac{3}{2}}}{\hat{\nu}_{13}} [\ln(1/\eta_*) - 1] dy. \quad (8.6)$$

The logarithmic factor means that  $\Gamma$  will be moderately large, in the range 15–25 depending upon the shape and roughness of the estuary bed.

An attractive feature of the representation (8.5) is that it clearly reveals time, lateral and vertical structure of the longitudinal velocity profile. The corresponding representation for the vertical eddy diffusivities is

$$\nu_{13} = \hat{\nu}_{13} \Gamma^{-1} \bar{h} \langle |U_0| \rangle (h/\bar{h})^{\frac{3}{2}} (1 - \eta) \eta, \quad (8.7)$$

i.e. diffusivity proportional to the three-halves power of the local water depth. For completeness we note that for the transverse turbulent mixing coefficient  $\kappa_2$  the representation is

$$\kappa_2 = \hat{\kappa}_2 \Gamma^{-1} \bar{h} \langle |U_0| \rangle (h/\bar{h})^{\frac{3}{2}} \eta^{\frac{1}{2}}, \quad (8.8)$$

where the dimensionless empirical constant  $\hat{\kappa}_2$  is approximately 0.2 (Fischer 1973).

The key results (8.5), (8.7) now make it straightforward for us to evaluate the formulae (6.3)–(6.10) concerning the detailed structure of the flow field and the transverse concentration distribution. First, we perform the triple integration (6.3) and obtain the stream function for the buoyancy-driven secondary flow:

$$\psi_0 = \frac{\beta g \partial_y s_0 \bar{h}^3 \Gamma}{4 \hat{\nu}_{23} \langle |U_0| \rangle} (h/\bar{h})^{\frac{3}{2}} \left\{ \eta(1 - \eta) - \frac{\eta \ln \eta}{[\ln(1/\eta_*) - 1]} \right\}. \quad (8.9)$$

Already we are in a position to calculate the components  $D_0$ ,  $D_1$  and  $K$  of the local dispersion matrix. This merely entails the evaluation of the vertical integrals (7.9), (7.10), (7.11). Unfortunately, all three dispersion coefficients involve the non-elementary definite integral

$$\int_0^1 \frac{\eta (\ln \eta)^2}{1 - \eta} d\eta = 2 \sum_{n=2}^{\infty} n^{-3} = 0.4041 \quad (8.10)$$

(Elder 1959). Thus, the results are rendered less attractive by the occurrence of decimal terms

$$D_0 = \frac{0.4041 U_0^2 \bar{h}}{\Gamma \hat{\nu}_{13}^2 \hat{\kappa}_3 \langle |U_0| \rangle} (h/\bar{h})^{\frac{3}{2}}, \quad (8.11)$$

$$D_1 = \frac{\beta g \partial_y s_0 \Gamma U_0 \bar{h}^3}{16 \hat{\nu}_{13} \hat{\nu}_{23} \hat{\kappa}_3 \langle |U_0| \rangle^2} (h/\bar{h})^{\frac{3}{2}} \left\{ 1 - \frac{1.6164}{[\ln(1/\eta_*) - 1]} \right\}, \quad (8.12)$$

$$K = \frac{3}{4} \hat{\kappa}_2 \Gamma^{-1} \langle |U_0| \rangle \bar{h} (h/\bar{h})^{\frac{3}{2}} + \frac{(\beta g \partial_y s_0)^2 \Gamma^3 \bar{h}^5 (h/\bar{h})^{\frac{3}{2}}}{\langle |U_0| \rangle^3 96 \hat{\nu}_{23}^2 \hat{\kappa}_3} \left\{ 1 - \frac{3}{[\ln(1/\eta_*) - 1]} + \frac{2.4246}{[\ln(1/\eta_*) - 1]^2} \right\}. \quad (8.13)$$

Also, from the definition (7.13) we note that the dimensionless measure  $q$  of the oscillatory transverse shear is given by

$$q = \int_0^{\tau} U_0 d\tau \left\{ \frac{\partial_y h [\ln(1/\eta_*) - 1]}{2 \Gamma \hat{\nu}_3 \bar{h} (h/\bar{h})^{\frac{3}{2}}} - \frac{(h/\bar{h})^{\frac{1}{2}} \partial_y \eta_*}{\Gamma \hat{\nu}_{13} \eta_*} \right\}. \quad (8.14)$$

All these results are considerably simplified if instead of neglecting powers of  $\eta_*$  we make the stronger assumption that the roughness height is so small that the reciprocal of  $[\ln(1/\eta_*) - 1]$  is negligible. (From the definition (8.6) it would also follow that  $\Gamma^{-1}$  is negligible.)

Next, we infer from equation (6.4) that the oscillatory part of the leading-order concentration perturbation is given by

$$c'_0 = \partial_{\xi} \bar{c} \int_0^{\tau} U_0 d\tau \left\{ 1 - \frac{(h/\bar{h})^{\frac{1}{2}} [\ln(1/\eta_*) - 1]}{\Gamma \hat{\nu}_{13}} \right\}. \quad (8.15)$$

As with all the results for the contaminant distribution, this result is equally applicable to the salinity distribution. Thus, in equation (8.9) for the secondary flow it is only the steady contribution  $\langle \partial_y s_0 \rangle$  to the transverse salinity gradient  $\partial_y s_0$  that remains to be determined (i.e.  $(\partial_y s_0)' = -q \partial_{\xi} \bar{s}$ ). In particular, it follows from equations (8.15) and (8.9) that  $\psi_0$  is exactly out of phase with the leading-order tidal current  $u_0$ . Furthermore, both  $\langle D_1 \rangle$  and  $\langle D_1 q \rangle$  are identically zero.

Proceeding to equation (6.5) for the vertical concentration gradient, and then using that result in the formula (5.10), we arrive at an expression for the vertical gradient Richardson number:

$$Ri_1 = -\frac{\beta g \partial_{\xi} \bar{s} \bar{h}^2}{U_0 \langle |U_0| \rangle} \Gamma^2 \frac{\hat{\nu}_{13}}{\hat{\kappa}_3} (h/\bar{h}) \frac{\eta^2 \ln \eta}{1 - \eta} + \left( \frac{\beta g \partial_y s_0 \bar{h}^2}{U_0 \langle |U_0| \rangle} \right)^2 \frac{\Gamma^4 \hat{\nu}_{13}^2}{\hat{\kappa}_3 \hat{\nu}_{23}} (h/\bar{h})^2 \left\{ \eta^2 - \frac{\eta^2 \ln \eta}{1 - \eta} \frac{1}{[\ln(1/\eta_*) - 1]} \right\}. \quad (8.16)$$

We notice that at the turn of the tide  $Ri_1$ , and hence  $(\nu_{13})_1$ , becomes singular. Thus, for a brief span of time the formula (6.6) for the perturbed eddy viscosity is inapplicable. Fortunately, for the limited needs of the present study, the results do not depend upon the way in which the singularity in  $(\nu_{13})_1$  is removed. Indeed, if  $\ln(1/\eta_*)$  is very large then it turns out that Richardson-number effects could have been totally ignored.

We now have sufficient information (8.5), (8.7), (8.9), (8.16) to solve equation (6.10) for the order  $\delta$  correction  $u_1$  to the longitudinal velocity. The singularity of strength  $U_0^{-2}$  in  $(\nu_{13})_1$  leads to a weaker  $U_0^{-1}$  singularity in  $u_1$ . However, when we calculate tidal averages this term makes no contribution, provided that Cauchy principal values are taken of the singular time-integral. If, instead, we had resolved the singularity and  $(\nu_{13})_1$  became very large but finite, then the contribution from this term would not necessarily be exactly zero but nevertheless be very small. The weaker  $U_0^{-1}$  singularity in  $Ri_1$  goes over to a non-singular (and non-zero) term in  $u_1$  and presents no difficulties. The full expression for the residual current is

$$\langle \|u_1\| \rangle = -\frac{g \bar{h} \langle \partial_{\xi} \bar{s}_1 \rangle}{\hat{\nu}_{13} \langle |U_0| \rangle} \Gamma (h/\bar{h})^{\frac{1}{2}} [\ln(1/\eta_*) - 1] - \frac{\beta g \partial_{\xi} \bar{s} \bar{h}^2}{\hat{\nu}_{13} \langle |U_0| \rangle} \Gamma (h/\bar{h})^{\frac{3}{2}} [\ln(1/\eta_*) - \frac{3}{2}] + \frac{5}{8} \frac{\beta g \partial_{\xi} \bar{s} \bar{h}^2}{\hat{\kappa}_3 \langle |U_0| \rangle} \Gamma (h/\bar{h})^{\frac{3}{2}}, \quad (8.17)$$

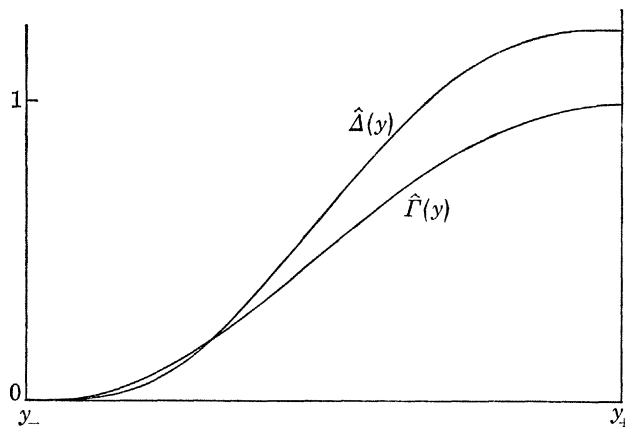
where the three contributions correspond to the first three terms in equation (6.10).

We recall that the residual slope  $\langle \partial_{\xi} \bar{s}_1 \rangle$  of the free surface is to be determined so that there is no net flow associated with the buoyancy-driven current. This constraint leads us to generalize the definition (8.5):

$$\hat{F}(y) \Gamma = \frac{1}{y_+ - y_-} \int_{y_-}^{y_+} \frac{(h/\bar{h})^{\frac{3}{2}}}{\hat{\nu}_{13}} [\ln(1/\eta_*) - 1] dy, \quad (8.18)$$

and to introduce a further non-dimensional function

$$\hat{A}(y) \Gamma = \frac{1}{y_+ - y_-} \int_{y_-}^{y_+} \frac{(h/\bar{h})^{\frac{3}{2}}}{\hat{\nu}_{13}} \left[ \ln(1/\eta_*) - \frac{3}{2} + \frac{5}{8} \frac{\hat{\nu}_{13}}{\hat{\kappa}_3} \right] dy \quad (8.19)$$

FIGURE 7. Graphs of the functions  $\hat{F}(y)$  and  $\hat{A}(y)$ .

(see figure 7). In terms of  $\hat{F}(y)$  and  $\hat{A}(y)$  the salinity-induced free-surface slope along the estuary is given by

$$g\langle\partial_{\xi}\bar{\zeta}_1\rangle = -\beta g\partial_{\xi}\bar{s}\hat{A}(y_+), \quad (8.20)$$

and the tidally-averaged stream function for the horizontal circulation has the representation

$$\langle\Phi\rangle = \frac{\beta g\partial_{\xi}\bar{s}\Gamma^2}{\langle|U_0|\rangle} \bar{h}^2 A_0 \{\hat{A}(y_+) \hat{F}(y) - \hat{A}(y)\}. \quad (8.21)$$

The Richardson-number effect is represented via the  $(\hat{v}_{13}/\hat{\kappa}_3)$  term in the definition (8.19) of  $\hat{A}(y)$ . Thus, if the roughness height is so small that  $\ln(1/\eta_*)$  is a large quantity, then, for the class of estuaries being studied here, Richardson-number effects can be ignored. It deserves emphasis that the negligibility of this physical effect is principally related to the phase and not to the size of the terms.

Close to the right-hand shoreline  $y = y_-$  where the water is extremely shallow, we can infer that the function  $\hat{F}(y)$  initially grows as  $(h/\bar{h})^{\frac{1}{2}}$  and that  $\hat{A}(y)$  is smaller still by order  $(h/\bar{h})$ . Thus, when  $y - y_-$  is small it follows that  $\langle\Phi\rangle$  is positive and increasing – hence that the residual flow is seawards. A similar argument enables us to deduce that, close to the opposite bank,  $\langle\Phi\rangle$  is negative and increasing. Again the flow is seawards. The physical interpretation is that, in accord with intuition, the saltier water tends to intrude upstream in the deeper central part of an estuary and the compensating downstream flow of fresher water occurs in the shallows (see figure 6).

Finally, we consider equation (7.14), or equivalently equation (6.9) for the quasi-steady concentration gradient across the estuary. Using the above results (8.12), (8.13), (8.14), (8.21) and most crucially the equation (8.15) for the oscillatory part of the salinity gradient, we arrive at the equation

$$\begin{aligned} \langle\partial_y c_0\rangle & \left[ \frac{3}{4}\hat{\kappa}_2 + \left( \frac{\beta g\langle\partial_y s_0\rangle \bar{h}^2 \Gamma^2}{\langle|U_0|\rangle^2} \right)^2 \frac{(h/\bar{h})^2}{96\hat{\kappa}_3\hat{p}_{23}^2} + \left( \frac{\beta g\partial_{\xi}\bar{s}\bar{h}^2 \Gamma^2}{\langle|U_0|\rangle^2} \right)^2 \frac{(h/\bar{h})^2}{96\hat{\kappa}_3\hat{p}_{23}^2} \langle q^2 \rangle \right] \\ & = \partial_{\xi}\bar{c} \left[ \left( \frac{\beta g\partial_{\xi}\bar{s}\bar{h}^2 \Gamma^2}{\langle|U_0|\rangle^2} \right) \left\{ \frac{\hat{A}(y_+) \hat{F}(y) - \hat{A}(y)}{(h/\bar{h})^{\frac{1}{2}}} \right\} \frac{A_0 \Gamma}{\bar{h}^2} \right. \\ & \quad \left. - 2 \left( \frac{\beta g\langle\partial_y s_0\rangle \bar{h}^2 \Gamma^2}{\langle|U_0|\rangle^2} \right) \left( \frac{\beta g\partial_{\xi}\bar{s}\bar{h}^2 \Gamma^2}{\langle|U_0|\rangle^2} \right) \frac{(h/\bar{h})^2}{96\hat{\kappa}_3\hat{p}_{23}^2} \langle q^2 \rangle \right]. \quad (8.22) \end{aligned}$$

For clarity, a common factor  $\langle |U_0| \rangle \bar{h}^2 (h/\bar{h})^{3/2} / \Gamma$  and additional terms involving inverse powers of  $[\ln(1/\eta_*) - 1]$  have been omitted.

Of particular interest in the present context is the role of buoyancy. From the left-hand side terms of equation (8.22) we can infer that both the steady and the oscillatory transverse salinity gradients augment the tidally-averaged dispersion across the estuary, and therefore tend to reduce the steady transverse concentration gradient  $\langle \partial_y c_0 \rangle$ . Similarly, on the right-hand side the quadratic salinity term has the opposite sign to the residual current term, so also tends to reduce  $\langle \partial_y c_0 \rangle$ . The physical origin of this quadratic term is the tidally-averaged dispersion across the estuary of the oscillatory concentration perturbation. When the tide is on the ebb the oscillatory contribution to the salinity is of the same sense as the steady transverse gradient (i.e. saltier at the centre of the estuary). Thus, the secondary flow and shear dispersion across the estuary are particularly strong. For the same reason the total transverse concentration gradient  $\partial_y c'_0 + \langle \partial_y c_0 \rangle$  is also large. This coincidence of strong gradients and strong dispersion greatly increases the net transverse mixing. As with all quadratic effects, the flood tide with its weak gradients and weak dispersion across the estuary, does not fully cancel out the increased mixing. Hence, as has already been stated, the overall effect of this tidal-oscillation term is to reduce  $\langle \partial_y c_0 \rangle$ .

For the important special case, in which salt is the contaminant being studied, equation (8.22) ceases to be linear. With an eye upon the way in which the equation is subsequently used, we re-arrange and non-dimensionalize the terms:

$$\begin{aligned} & \left( \frac{\beta g \langle \partial_y s_0 \rangle \bar{h}^2 \Gamma^2}{\langle |U_0| \rangle^2} \right) \left[ \frac{3}{2} \hat{\kappa}_2 + 3 \left( \frac{(\beta g \partial_{\xi} \bar{s})^2 \bar{h}^2 A_0 \Gamma^5}{\langle |U_0| \rangle^4} \right) \frac{(h/\bar{h})^2}{96 \hat{\nu}_{23}^2 \hat{\kappa}_3} \left\langle \frac{q^2 \bar{h}^2}{A_0 \Gamma} \right\rangle \right] + \left( \frac{\beta g \langle \partial_y s_0 \rangle \bar{h}^2 \Gamma^2}{\langle |U_0| \rangle^2} \right)^3 \frac{(h/\bar{h})^2}{96 \hat{\nu}_{23}^2 \hat{\kappa}_3} \\ & = \left( \frac{(\beta g \partial_{\xi} \bar{s})^2 \bar{h}^2 A_0 \Gamma^5}{\langle |U_0| \rangle^4} \right) \left\{ \frac{\hat{\Delta}(y_+) \hat{\Gamma}(y) - \hat{\Delta}(y)}{(h/\bar{h})^{3/2}} \right\}. \quad (8.23) \end{aligned}$$

This is a cubic equation for  $\langle \partial_y s_0 \rangle$ . Fortunately, the positivity of the coefficients on the left-hand side ensures that there is a unique real solution. Moreover, the sign of  $\langle \partial_y s_0 \rangle$  is the same as that of the horizontal stream function  $\langle \Phi \rangle$ . Thus, the tidally averaged salinity is indeed greater in the deeper water at the centre of an estuary than it is in the shallower water at the sides.

## 9. DISPERSION COEFFICIENTS

A basic requirement for a classification scheme is that the results should be expressed in terms of appropriate dimensionless combinations of physical quantities. For example, the scalings employed in the nonlinear equation (8.23) were motivated by the facts that the importance of tidal oscillation effects is thereby indicated by the single factor  $\langle q^2 \bar{h}^2 / A_0 \Gamma \rangle$ , and that the coefficients of the remaining three terms are of order unity. Also, it is preferable that the magnitude of the dimensionless parameters should indicate the relative importance of the corresponding physical effect. For example, the repeated occurrence of the large quantity  $\Gamma$  throughout the above analysis means that it is desirable that the chosen parameters should include appropriate powers of  $\Gamma$ . It was for this reason that the functions  $\hat{\Gamma}(y)$  and  $\hat{\Delta}(y)$  were rendered of order unity by the inclusion of  $\Gamma$  factors in the definitions (8.18), (8.19).

These considerations lead us to define two parameters  $F$  and  $G$  associated respectively with the importance of flow oscillations and of the longitudinal density gradient:

$$F = \frac{\bar{h} \langle |U_0| \rangle^2}{B^3 \omega^2 \Gamma}, \quad G = \frac{(\beta g \partial_{\xi} \bar{s})^2 \bar{h}^3 B \Gamma^5}{\langle |U_0| \rangle^4}. \quad (9.1)$$

Here  $\omega$  is the tidal frequency and  $2B = y_+ - y_-$  is the local estuary width. As noted above, the tidal effect in the transverse dispersion equation (8.23) is measured by the factor  $\langle q^2 \bar{h}^2 / A_0 \Gamma \rangle$ . From equation (8.14) and the definition (9.1) of  $F$ , we find that

$$q = F^{1/2} (\Gamma B / h)^{1/2} \hat{q} \sin(\omega\tau + \chi) \quad (9.2)$$

with

$$\hat{q} = \frac{\pi B \partial_y (h/\bar{h}) [\ln(1/\eta_*) - 1]}{4 (h/\bar{h})^{1/2} \hat{\nu}_{13} \Gamma}, \quad (9.3)$$

where additional terms of order  $\Gamma^{-1}$  have been neglected, and we have made explicit use of the hypothesis (vi) that the tidal current is sinusoidal. It now follows that

$$\langle q^2 \bar{h}^2 / A_0 \Gamma \rangle = \frac{1}{4} F \hat{q}^2. \quad (9.4)$$

Since the function  $\hat{q}$  is of order unity, the parameter  $F$  is indeed a direct measure of the importance of flow oscillations. Similarly, the buoyancy parameter  $G$  stems from the scalings adopted in equation (8.23), with the obvious substitution  $2B\bar{h}$  for the cross-sectional area  $A_0$ . For subsequent convenience, we rewrite equation (8.23)

$$r \left[ \frac{3}{4} \hat{\kappa}_2 + \frac{3}{2} n F G \hat{q}^2 (h/\bar{h})^2 \right] + n r^3 (h/\bar{h})^2 = 2G \left\{ \frac{\hat{\Delta}(y_+) \hat{\Gamma}(y) - \hat{\Delta}(y)}{(h/\bar{h})^{3/2}} \right\}, \quad (9.5)$$

where  $n = 1/96 \hat{\kappa}_3 \hat{\nu}_{23}^2$  and  $r$  denotes a Richardson number associated with transverse, rather than vertical, density gradients

$$r = \beta g \langle \partial_y s_0 \rangle \bar{h}^2 \Gamma^2 / \langle |U_0| \rangle^2. \quad (9.6)$$

The selection of parameters (9.1) implies that the appropriate non-dimensionalization of the contribution  $E_S, E_T$  to the longitudinal dispersion coefficient is

$$E_S = B \langle |U_0| \rangle \hat{E}_S(F, G), \quad E_T = B \langle |U_0| \rangle \hat{E}_T(F, G), \quad (9.7)$$

where the circumflexes  $\hat{\phantom{x}}$  are used to signify non-dimensional quantities, which are formally of order unity. The actual size depends, of course, upon the local estuarine parameters  $F$  and  $G$ . The non-dimensional analogues of the dispersion formulae (7.15), (7.16) are

$$\hat{E}_S = \frac{G}{2B} \int_{y_-}^{y_+} \frac{4 \{ \hat{\Delta}(y_+) \hat{\Gamma}(y) - \hat{\Delta}(y) \}^2 dy}{\left[ \frac{3}{4} \hat{\kappa}_2 + \frac{1}{2} n F G \hat{q}^2 (h/\bar{h})^2 + n r^2 (h/\bar{h})^2 \right] (h/\bar{h})^{5/2}}, \quad (9.8)$$

$$\hat{E}_T = \frac{F}{2B} \int_{y_-}^{y_+} \frac{\left[ \frac{3}{8} \hat{\kappa}_2 + \frac{3}{8} n F G \hat{q}^2 (h/\bar{h})^2 + \frac{1}{2} n r^2 (h/\bar{h})^2 \right] \hat{q}^2 (h/\bar{h})^{5/2} dy}{\left[ \frac{3}{4} \hat{\kappa}_2 + \frac{1}{2} n F G \hat{q}^2 (h/\bar{h})^2 + n r^2 (h/\bar{h})^2 \right]^{3/2}} dy. \quad (9.9)$$

The functions  $\hat{\Gamma}, \hat{\Delta}, \hat{q}, r$  involved in these expressions are defined in equations (8.18), (8.19), (9.3), (9.5) respectively, and  $n = 1/96 \hat{\nu}_{23}^2 \hat{\kappa}_3$ .

For weak buoyancy we can confirm analytically Macqueen's (1978*a*, 1979) deduction that in wide estuaries the effect of salt is to increase the longitudinal dispersion coefficient. To do this, we seek Taylor's series expansions for  $r$ , and hence for  $\hat{E}_S$  and  $E_T$  in powers of  $G$ . The resulting expression for the total (non-dimensional) dispersion coefficient due to steady and to oscillatory transverse shears is

$$\hat{E}_S + \hat{E}_T = \frac{F}{2B} \int_{y_-}^{y_+} \frac{3}{8} \hat{\kappa}_2 \hat{q}^2 (h/\bar{h})^{5/2} dy + \frac{F^2 G}{2B} \int_{y_-}^{y_+} \frac{3}{8} n \hat{q}^4 (h/\bar{h})^{5/2} dy + \frac{G}{2B} \int_{y_-}^{y_+} \frac{4 \{ \hat{\Delta}(y_+) \hat{\Gamma}(y) - \hat{\Delta}(y) \}^2 dy}{\frac{3}{4} \hat{\kappa}_2 (h/\bar{h})^{5/2}} dy + O(G^3). \quad (9.10)$$

Since the integrands are all positive and  $G$  is positive by definition, it follows that weak buoyancy increases the dispersion. The  $F^2G$  term represents the interaction between tidal and buoyancy effects, and is related to that part of the secondary flow that is driven by the oscillatory transverse salinity gradient. The  $G$  term is associated with the steady horizontal circulation and therefore would be ignored in Macqueen's (1978*a*, 1979) analysis.

Remarkably, the approximation (9.10) to the non-dimensional dispersion coefficient is valid over a substantial range of the estuarine parameters. First, it happens that the  $G^2$  term in the Taylor's series is zero. Also, in either of the limits of large  $G$  or of large  $F$  the first three terms in an asymptotic expansion for the dispersion are

$$\hat{E}_S + \hat{E}_T = \frac{F^2G}{2B} \int_{y_-}^{y_+} \frac{3}{8} n \hat{q}^4 (h/\bar{h})^{\frac{3}{2}} dy + \frac{F}{2B} \int_{y_-}^{y_+} \frac{3}{8} \hat{\kappa}_2 \hat{q}^2 (h/\bar{h})^{\frac{3}{2}} dy + \frac{1}{2BF} \int_{y_-}^{y_+} \frac{16}{3n} \frac{\{\hat{A}(y_+) \hat{F}(y) - \hat{A}(y)\}^2}{\hat{q}^2 (h/\bar{h})^{\frac{3}{2}}} dy. \quad (9.11)$$

Thus, for large  $G$  the dominant  $F^2G$  term agrees with equation (9.10) and the error is of order unity, while for large  $F$  both the  $F^2G$  and  $F$  terms are correct and the error is only of order  $F^{-1}$ . Hence, it is only for small  $F$  with moderate values of  $F^2G$  that the approximation (9.10) is suspect. Since the density gradient parameter is quadratic in  $\partial_y \bar{s}$ , it follows that the dispersion equation (7.1) is approximated by the Erdogan–Chatwin equation (Erdogan & Chatwin 1967, see also Smith 1978*b*).

To obtain quantitative results we must specify the cross-sectional shape and the bottom roughness across the estuary. For reasons of tractability we model  $\ln(1/\eta_*)$  as being constant. Thus, the Chezy coefficient  $\Gamma$  is given by

$$\Gamma = (\overline{h^{\frac{3}{2}}}/\bar{h}^{\frac{3}{2}}) [\ln(1/\eta_*) - 1]/\hat{\nu}_{13}, \quad (9.12)$$

where the overbar denotes the cross-sectional average value. Using this result in equations (8.18), (8.19), (9.2), we obtain the expressions

$$\hat{F}(y) = \frac{1}{2B} \int_{y_-}^y (h^{\frac{3}{2}}/\bar{h}^{\frac{3}{2}}) dy, \quad (9.13)$$

$$\hat{A}(y) = \frac{1}{2B} \int_{y_-}^y (h^{\frac{3}{2}}/\bar{h}^{\frac{3}{2}}) dy, \quad (9.14)$$

$$\hat{q}(y) = \frac{1}{4} \pi B \partial_y h \bar{h} / h^{\frac{3}{2}} \bar{h}^{\frac{3}{2}}, \quad (9.15)$$

where, for consistency with the use of equation (8.23), we have neglected additional terms of order  $\Gamma^{-1}$ . For example, the vertical stratification ( $\hat{\nu}_{13}/\hat{\kappa}_3$ ) contribution to  $\hat{A}(y)$  is ignored (see the discussion following equation (8.21)). Substituting the expression (9.13), (9.14), into equation (8.21) for the horizontal stream function  $\langle \Phi \rangle$ , and then differentiating with respect to  $y$ , we obtain the result

$$\langle \|u_1\| \rangle = \langle |U_0| \rangle \frac{G^{\frac{1}{2}} \bar{h}^{\frac{1}{2}}}{B^{\frac{1}{2}} \bar{h}^{\frac{3}{2}}} h^{\frac{1}{2}} \left( \frac{\bar{h}^{\frac{3}{2}}}{h^{\frac{3}{2}}} - h \right). \quad (9.16)$$

Thus, the steady upstream intrusion of saltier water is confined to those parts of the estuary where the local water depth exceeds  $\bar{h}^{\frac{3}{2}}/h^{\frac{3}{2}}$ . Also, the upstream residual velocity is greatest at the deepest part of the estuary, while the maximum downstream residual current occurs where the water depth is  $\frac{1}{3} \bar{h}^{\frac{3}{2}}/h^{\frac{3}{2}}$ .

For an estuary of parabolic cross-section

$$h = \frac{3}{2}\bar{h}[1 - (y/B)^2], \quad -B \leq y \leq B, \tag{9.17}$$

(see figure 8) the integrals and cross-sectional average values can be evaluated explicitly. In particular, we record that

$$\bar{h}^{\frac{3}{2}} = \frac{3}{16}\pi(\frac{3}{2}\bar{h})^{\frac{3}{2}}, \quad \bar{h}^{\frac{5}{2}} = \frac{5}{16}\pi(\frac{3}{2}\bar{h})^{\frac{5}{2}}, \tag{9.18}$$

$$\hat{q}(y) = -\frac{16}{9}(y/B)[1 - (y/B)^2]^{-\frac{1}{2}}, \tag{9.19}$$

$$\hat{\Delta}(y_+) \hat{\Gamma}(y) - \hat{\Delta}(y) = -\frac{2}{3}\pi^{-1}(y/B)[1 - (y/B)^2]^{\frac{5}{2}}, \tag{9.20}$$

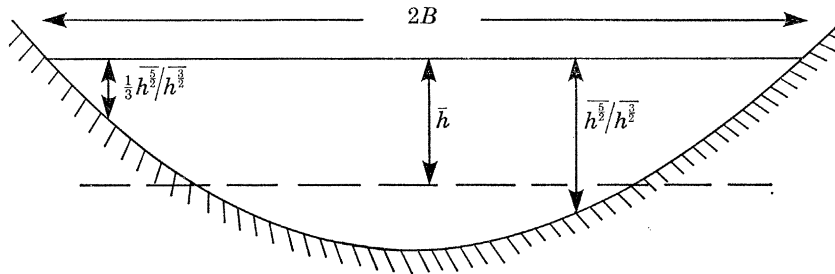


FIGURE 8. Definition sketch for the cross-section used in the analysis.

and that the Taylor's series approximation (9.10) becomes

$$\hat{E}_S + \hat{E}_T = \frac{\pi\hat{\kappa}_2}{4\sqrt{6}}F + \frac{\pi F^2 G}{\hat{\nu}_{23}\hat{\kappa}_3 288\sqrt{6}} + \frac{5\sqrt{6}G}{3^6\pi\hat{\kappa}_2} = 0.064F + 0.070F^2G + 0.027G, \tag{9.21}$$

where we have taken  $\hat{\nu}_{23} = \hat{\kappa}_3 = 0.4$  and  $\hat{\kappa}_2 = 0.2$  (see equations (8.1), (8.8)).

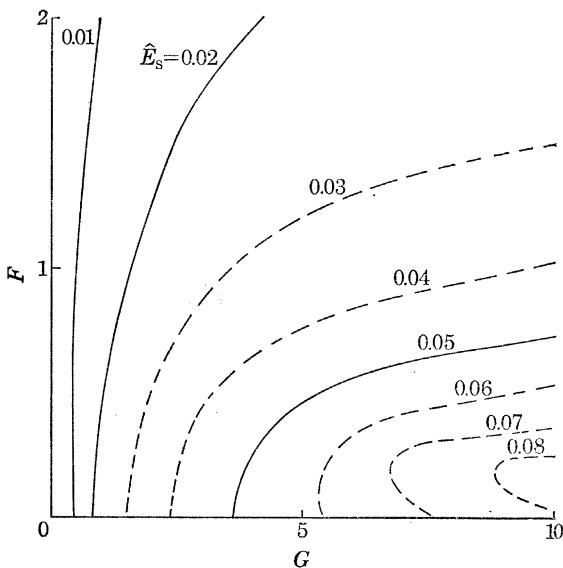


FIGURE 9

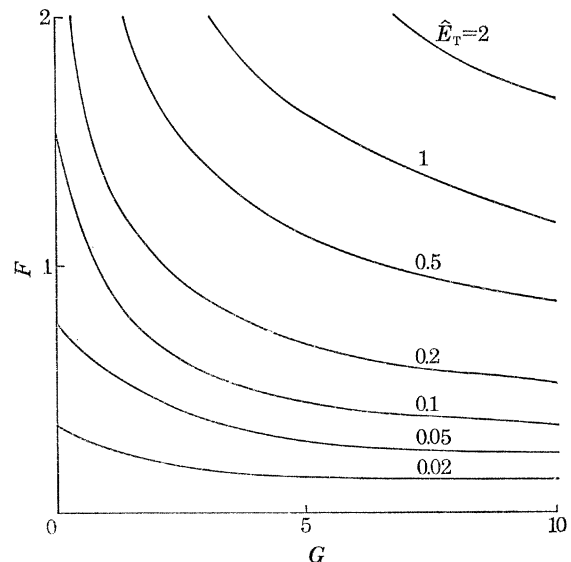


FIGURE 10

FIGURE 9. Contours of the steady buoyancy-driven contribution  $\hat{E}_S$  to the non-dimensional dispersion coefficient  $E/B\langle|U|\rangle$ .

FIGURE 10. Contours of the oscillatory transverse shear contribution  $\hat{E}_T$  to  $E/B\langle|U|\rangle$ .

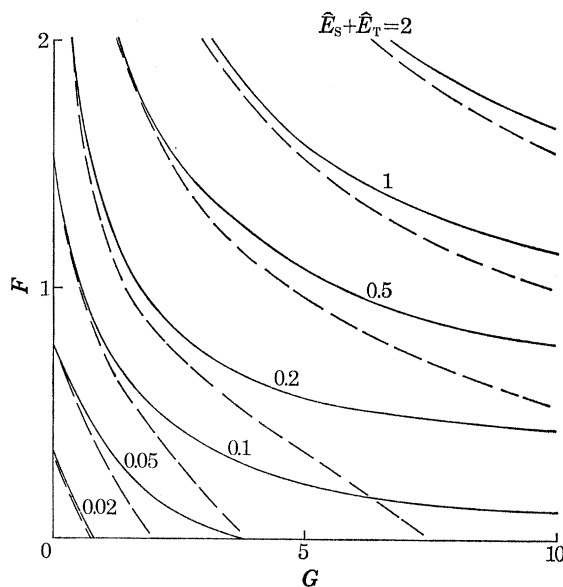


FIGURE 11. Contours, —, of  $\hat{E}_S + \hat{E}_T$  compared with the contours, ---, given by the 3-term Taylor's series approximation.

It is now a straightforward computational task to solve the cubic equation (9.3) and to evaluate the dimensionless contributions  $\hat{E}_S$  and  $\hat{E}_T$  to the longitudinal dispersion coefficient. Figures 9 and 10 respectively give contours of  $\hat{E}_S$  and  $\hat{E}_T$  as functions of the flow oscillation and density gradient parameters for wide estuaries with parabolic-depth profiles. We observe that  $\hat{E}_S$  is principally a function of the density gradient and tends to be reduced by flow oscillation effects, while  $\hat{E}_T$  is principally related to the tidal current and is increased by salinity effects. Figure 11 gives a comparison between the contours of  $\hat{E}_S + \hat{E}_T$  as given by the numerical results and by the Taylor's series (9.21). In accord with the above deductions, the simple approximation is tolerably accurate over a wide range.

For the third significant contribution,  $E_V$ , to the longitudinal dispersion coefficient, the only non-zero term in the expression (7.17) is the Elder (1959)  $D_0$  term. Thus, using equation (8.11) for  $D_0$ , and assuming that the tidal current  $U_0$  is sinusoidal, we arrive at the result

$$E_V = 0.4041 \left(\frac{1}{8}\pi^2\right) (h^{\frac{5}{2}}/h^{\frac{3}{2}}) \langle |U_0| \rangle \bar{h} / \Gamma \hat{\nu}_{13}^2 \hat{\kappa}_3, \quad (9.22)$$

i.e. the generalization of Bowden's (1965) results to estuaries of non-constant depth. If we take the estuary to have a parabolic cross-section, and  $\hat{\kappa}_3$  and  $\hat{\nu}_{13}$  both to have the value of 0.4, then we obtain

$$E_V = 10.5 \bar{h} \langle |U_0| \rangle / \Gamma. \quad (9.23)$$

#### 10. A CLASSIFICATION SCHEME FOR DISPERSION MECHANISMS

The scaling of  $E_V$ , equation (9.22), is different from that of  $E_S$  and of  $E_T$ , equation (9.7), because the vertical shear dispersion does not depend upon the estuary breadth  $2B$ . However, to permit a direct comparison between the importance of the buoyancy, flow oscillations, and vertical shear effects, we represent the longitudinal dispersion coefficient by the formula

$$E = B \langle |U_0| \rangle \{ (10.5/\Gamma^2) (\Gamma \bar{h}/B) + 0.064F + 0.070F^2G + 0.027G \}. \quad (10.1)$$



The artifice of including the  $\Gamma$  factor in the vertical shear parameter  $\Gamma\bar{h}/B$  ensures that the numerical coefficients are all of a comparable magnitude. For example, with  $\Gamma = 20$  the coefficient of  $\Gamma\bar{h}/B$  in equation (10.1) is 0.026. Thus, to a first approximation the dominant physical mechanism controlling the long-term dispersion of contaminants or of salinity along a wide well-mixed estuary depends upon which of  $(\Gamma\bar{h}/B)$ ,  $F$ ,  $F^2G$  and  $G$  is the largest. The respective mechanisms are the oscillatory vertical shear (Bowden 1965), the oscillatory transverse shear (Okubo 1967), the interaction between tidal and cross-estuary buoyancy effects (Macqueen 1978 *b*), and the buoyancy-driven steady horizontal circulation (Imberger 1976).

The four dimensionless factors all have different dependence upon the estuary breadth  $2B$  (see the definitions (9.1) of  $F$  and  $G$ ). Thus, we can envisage circumstances in which each mechanism becomes dominant for some range of  $B$ . For example, if we specify

$$\bar{h} = 10 \text{ m}, \quad \langle |U_0| \rangle = 1.5 \text{ m s}^{-1}, \quad \beta g \partial_{\xi} \bar{s} = 5 \times 10^{-7} \text{ s}^{-2}, \quad \Gamma = 20, \quad (10.2)$$

then, for  $B$  less than 100 m the interaction term dominates; for wider estuaries, with  $B$  less than 800 m, the transverse oscillatory shear dominates; for still wider estuaries the vertical shear dominates; and finally for  $B$  in excess of 1000 m the steady circulation is the principal dispersion

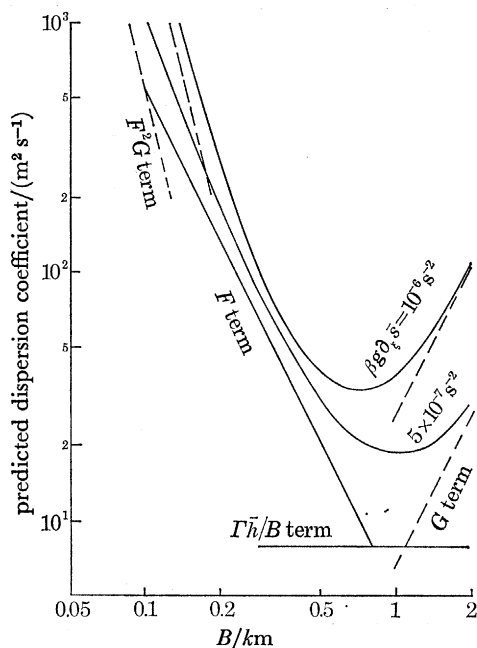


FIGURE 12. The longitudinal dispersion coefficient  $E$  as a function of the estuary width for the conditions given in equation (10.2) and also for the case with twice as large a salinity gradient.

mechanism. Figure 12 shows the predicted dispersion coefficient as a function of  $B$ , together with the results for double the longitudinal salinity gradient.

An important restriction upon the applicability of the above results is the requirement that the estuary be wide. We recall that for contaminant dispersion, an estuary is defined as being wide if the time scale for cross-sectional mixing exceeds the tidal period. From the formula (8.13) for the transverse dispersion coefficient this condition can be written

$$B^2 \cdot \frac{\Gamma}{\bar{h} \langle |U_0| \rangle \left[ \frac{3}{4} \kappa_2 + \frac{1}{2} n F G + G^{\frac{2}{3}} \right]} > \frac{2\pi}{\omega}, \quad (10.3)$$

where  $n = 1/96\hat{\nu}_{23}^2\hat{\kappa}_3 = 0.163$  and the  $G^{\frac{3}{2}}$  term allows for the circumstance in which  $G$  is large but  $F$  is extremely small. Using the definition (9.1) of  $F$ , we rewrite the constraint (10.3)

$$(\Gamma h/B)^{\frac{1}{2}} F^{\frac{1}{2}} [\frac{3}{4}\hat{\kappa}_2 + \frac{1}{2}nFG + G^{\frac{3}{2}}] < \Gamma/2\pi. \quad (10.4)$$

This requirement is quite stringent since it applies when the three estuarine parameters  $F$ ,  $G$ ,  $(\Gamma h/B)$  have values of order unity. In particular, for the illustrative example used above, the predictions are invalid for  $B$  less than about 100 m (130 m in the doubled gradient case).

It deserves emphasis that the results derived in §§ 8 and 9 are not strictly quantitative. Errors of order  $\Gamma^{-1}$  have been incurred in the cross-stream dispersion equation (8.22), in the neglect of vertical stratification (9.14), and in taking the roughness height  $h\eta_*$  to be proportional to the local water depth (9.12). Also, the turbulence model (8.1) is a considerable simplification upon the actual time-dependent turbulence (Maxey 1978). However the greatest source of uncertainty lies in the strong dependence of the results upon the estuary shape and roughness. For example, if the estuary were triangular then equations (9.17)–(9.21) would need to be replaced by

$$h = 2\bar{h}(y/B) \quad \text{for } 0 \leq y \leq B, \quad h = 2\bar{h}[2 - (y/B)] \quad \text{for } B \leq y \leq 2B, \quad (10.5)$$

$$\bar{h}^{\frac{3}{2}} = \frac{2}{5}(2\bar{h})^{\frac{3}{2}}, \quad \bar{h}^{\frac{5}{2}} = \frac{2}{7}(2\bar{h})^{\frac{5}{2}}, \quad (10.6)$$

$$\hat{q}(y) = \frac{5}{16}\pi(y/B)^{-\frac{1}{2}} \quad \text{for } 0 \leq y \leq B, \quad (10.7)$$

$$\hat{A}(y_+) \hat{F}(y) - \hat{A}(y) = \frac{5}{7}[(y/B)^{\frac{5}{2}} - (y/B)^{\frac{7}{2}}] \quad \text{for } 0 \leq y \leq B, \quad (10.8)$$

$$\hat{E}_S + \hat{E}_T = \frac{\pi^2 15\sqrt{2}}{256} F - \left(\frac{5\pi}{16}\right)^4 \frac{\sqrt{2}}{56\hat{\nu}_{23}^2\hat{\kappa}_3} F^2 G + \frac{800\sqrt{2}G}{7^3 \cdot 3^3 \cdot 11 \cdot \hat{\kappa}_2} \quad (10.9)$$

and the final model equation (10.1) for the total longitudinal dispersion coefficient becomes

$$E = B \langle |U_0| \rangle \{ (12.6/\Gamma^2) (\Gamma h/B) + 0.16F + 0.37F^2G + 0.056G \}. \quad (10.10)$$

Thus, each coefficient is significantly larger than the corresponding coefficient for a parabolic estuary. Similarly, a relative error of  $\theta\%$  in the roughness height leads to errors of about  $-\frac{1}{2}\theta\%$  in the value of the density gradient parameter. Thus, the results of our model calculations are not sufficiently precise to replace field observations. Rather, they permit us to determine which physical mechanisms are dominant and hence how the dispersion coefficient scales when conditions are changed.

The above considerations are well illustrated if, following Macqueen (1978*a*), we take the physical parameters to have values appropriate to the Thames 30 km seawards of London Bridge (in the vicinity of the Littlebrook power station):

$$B = 350 \text{ m}, \quad \bar{h} = 10 \text{ m}, \quad \langle |U_0| \rangle = 1.16 \text{ m s}^{-1}, \quad \beta g \partial_x \bar{s} = 2.4 \times 10^{-6} \text{ s}^{-2}. \quad (10.11)$$

To determine the non-dimensional Chezy coefficient  $\Gamma$  we assume that the bed is smooth, so that locally, at any point across the estuary, the ratio  $\|u_0\|/u_*$  of the vertically averaged velocity to the friction velocity, is about 20,

$$\text{i.e.} \quad [\ln(1/\eta_*) - 1]/\hat{\nu}_{13} = 20. \quad (10.12)$$

If the estuary cross-section is parabolic, then it follows from equations (9.1), (9.2) and (9.12) that

$$\Gamma h/B = 0.62, \quad F = 0.74, \quad F^2G = 2.87, \quad G = 5.23, \quad (10.13)$$

and that the longitudinal dispersion coefficient is given by the sum

$$E = 5.3 + 18.4 + 81.5 + 72.0 = 177.2 \text{ m}^2 \text{ s}^{-1}. \quad (10.14)$$

Also, the wide-estuary condition (10.4) is indeed satisfied. On the other hand if, as was done by Macqueen (1978*a*), we model the cross section by an equilateral triangle, then we arrive at the result

$$E = 6.1 + 46.0 + 494.2 + 149.2 = 697.5 \text{ m}^2 \text{ s}^{-1}. \quad (10.15)$$

(Macqueen obtains the much larger value  $1820 \text{ m}^2 \text{ s}^{-1}$ , but as has already been pointed out, his method amounts to an interpolation formula and cannot be expected to be accurate when the interaction terms dominate). For average flow conditions the dispersion coefficient at Littlebrook, inferred from the salinity distribution, is about  $350 \text{ m}^2 \text{ s}^{-1}$  (Macqueen 1978*b*).

Despite the variation in the estimates (9.37) and (9.38) for  $E$  (a factor of two either side of the observed value), there is agreement on the fact that the physical mechanisms primarily responsible for longitudinal dispersion at that reach of the Thames are: the interaction between tidal and cross-estuary buoyancy effects and the buoyancy driven steady horizontal circulation. Since these  $F^2G$  and  $G$  terms dominate respectively for small and for large estuary widths, it follows that the same two terms will give the major contributions to the dispersion well upstream and downstream of Littlebrook. Thus, in the Thames downstream of London Bridge, the dispersion is strongly linked to the value of the local salinity gradient. However, contrary to the situation in narrow estuaries (Smith 1977), the effect of buoyancy is to increase the dispersion. Specifically, the length scale of the salinity intrusion up the estuary varies as the inverse one-third power of the freshwater discharge rate. Hence, even in a severe drought with an eightfold reduction in river run-off, the salinity would only penetrate about twice as far upstream as usual (i.e. wide buoyancy dominated estuaries, like the Thames downstream of London Bridge, are not particularly vulnerable to the effects of droughts). An equivalent characterization of the buoyancy-dominated régime is that the longitudinal dispersion coefficient varies as the two-thirds power of the fresh water discharge rate. Qualitatively this is similar to the observed behaviour of  $E$  in the Tay (Williams & West 1973), and in the Severn (Uncles & Radford 1980).

I wish to express my thanks to the following: Dr K. W. James for encouraging me to undertake research into the dispersion of solutes, Dr J. F. Macqueen for many helpful discussions, and the C.E.G.B. for financial support.

#### APPENDIX. AN ALTERNATIVE DERIVATION OF THE DISPERSION FORMULAE

In a recent study of transverse dispersion (Smith 1979), the author has derived a model equation that fairly accurately describes the horizontal dispersion of a buoyant solute in a steady, uniform, vertically well-mixed current. If we assume that essentially the same equation applies when the water is of non-uniform depth and when the current is unsteady, then we are led to consider the equation

$$\begin{aligned} (h + \zeta) \partial_t \|c\| + (h + \zeta) \|u\| \partial_x \|c\| + (h + \zeta) \|v\| \partial_y \|c\| + \partial_y \Phi \partial_x \|c\| - \partial_x \Phi \partial_y \|c\| \\ = (\partial_x, \partial_y) \begin{bmatrix} D_0 & D_1 \\ D_1 & K \end{bmatrix} \begin{bmatrix} (h + \zeta) \partial_x \|c\| \\ (h + \zeta) \partial_y \|c\| \end{bmatrix}. \quad (\text{A } 1) \end{aligned}$$

Here the dispersion coefficients  $D_0$ ,  $D_1$ ,  $K$  and the horizontal stream function  $\Phi$  are related to the detailed structure of the flow field by equations (7.9)–(7.12) above (equations (10*a*, *b*, *c*) and

(9d, e) of Smith 1979). The presence of the  $D_1$  terms indicates that, as a consequence of there being a secondary flow, the principal directions for maximum and minimum dispersion are not aligned along and across the estuary (see figure 13).

We now analyse equation (A 1) on the hypotheses

- (i) The estuary is much longer than the tidal excursions and the estuary width;
- (ii) Lateral mixing takes more than one tidal period.

The other major hypotheses (ii) (iv), (v) are implicit in the derivation of equation (A 1).

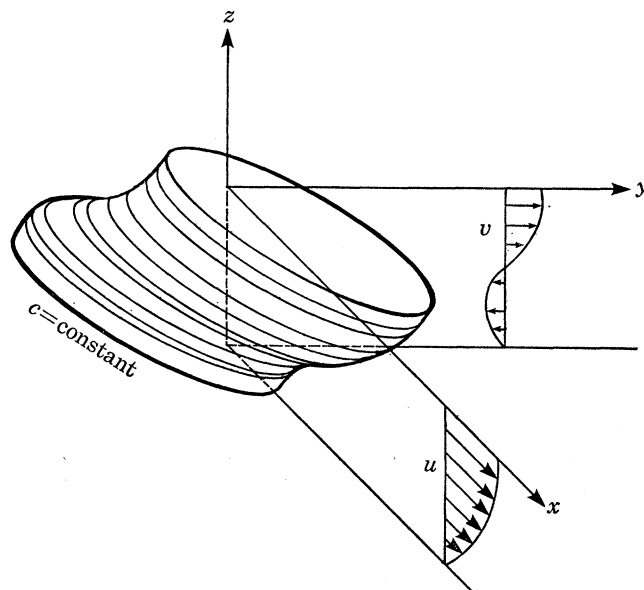


FIGURE 13. Perspective view of a concentration contour soon after contaminant release when there is a shear flow in two directions.

Proceeding as in § 3, we introduce a small parameter

$$\epsilon = \mathcal{B}/\mathcal{L}, \quad (\text{A } 2)$$

where  $\mathcal{B}$  and  $\mathcal{L}$  respectively are typical width and length scales for the estuary. Next, we take the transverse dispersion coefficient  $K$  to be of order  $\mathcal{B}\mathcal{U}\epsilon^\gamma$ , and the tidal frequency to be of order  $\mathcal{B}^{-1}\mathcal{U}\epsilon^\beta$ , where  $\mathcal{U}$  is a typical tidal velocity. Lengthy arguments of the type illustrated in figures 3 and 5 lead to the necessary scalings for the terms in equation (A 1) if maximum generality is to be achieved. Unlike the previous cases studied in this paper, the exponents  $\beta$  and  $\gamma$  remain undetermined except for the inequalities  $1, \gamma > \beta$  implied by the two hypotheses.

With the relative sizes of the terms made explicit, equation (A 1) can be written

$$\begin{aligned} & (h + \epsilon^{1-\beta}\zeta) \epsilon^{2+\gamma-\beta}\partial_x\|c\| + (h + \epsilon^{1-\beta}\zeta) \epsilon^\beta\partial_\tau\|c\| + (h + \epsilon^{1-\beta}\zeta) (\|u\|' + \epsilon^{1+\gamma-2\beta}\langle\|u\|\rangle) \epsilon\partial_x\|c\| \\ & + (h + \epsilon^{1-\beta}\zeta) \epsilon\|v\| \partial_y\|c\| + \partial_y(\epsilon^{\gamma-\beta}\Phi) \epsilon\partial_x\|c\| - \epsilon\partial_x(\epsilon^{\gamma-\beta}\Phi) \partial_y\|c\| \\ & = (\epsilon\partial_x, \partial_y) \begin{bmatrix} \epsilon^{\gamma-2\beta}D_0 & \epsilon^{\gamma-\beta}D_1 \\ \epsilon^{\gamma-\beta}D_1 & \epsilon^\gamma K \end{bmatrix} \begin{bmatrix} (h + \epsilon^{1-\beta}\zeta) \epsilon\partial_x\|c\| \\ (h + \epsilon^{1-\beta}\zeta) \partial_y\|c\| \end{bmatrix}. \quad (\text{A } 3) \end{aligned}$$

Here  $\epsilon^{-\beta}\tau$  is the tidal timescale (Cole 1968, ch. 3),  $\epsilon^{\beta-\gamma-2}T$  is the slow timescale associated with the long-term evolution of the contaminant distribution, and  $\langle\|u\|\rangle \epsilon^{1+\gamma-2\beta}$  is the relatively weak

non-tidal velocity associated with the freshwater discharge into the estuary (i.e. the tidal bulk-velocity  $\overline{\|u\|}$  has zero tidal average).

We shall arbitrarily set  $\beta = 0$ ,  $\gamma = 1$  in the following calculations. This has no effect upon the final conclusions, and has the minor convenience that equation (A 3) involves only integer powers of  $\epsilon$ . Thus, we seek solutions of the form

$$\|c\| = \|c\|^{(0)} + \epsilon \|c\|^{(1)} + \epsilon^2 \|c\|^{(2)} + \dots \quad (\text{A } 4)$$

At leading order in  $\epsilon$  we find that  $\|c\|^{(0)}$  is independent of the fast timescale  $\tau$ . Next, at order  $\epsilon$ , the tidally steady terms imply that  $\|c\|^{(0)}$  is uniform across the estuary, while the fluctuating terms yield the equation

$$\partial_\tau \|c\|^{(1)} = -\|u\|' \partial_x \|c\|^{(0)}. \quad (\text{A } 5)$$

Thus,  $\|c\|^{(0)}$  can be identified with the cross-sectionally averaged contaminant concentration  $\bar{c}$ , and the oscillatory transverse concentration gradient can be expressed

$$(\partial_y \|c\|^{(1)})' = -\partial_x \bar{c} \int_0^\tau \partial_y \|u\|' d\tau = -q \partial_x \bar{c}, \quad (\text{A } 6)$$

where  $q$ , as defined previously in equation (7.13), is a dimensionless measure of the oscillatory transverse shear.

Proceeding to order  $\epsilon^2$ , the steady terms give a transverse dispersion equation for the steady concentration gradient across the estuary

$$\partial_y (h \langle K \rangle \partial_y \langle \|c\|^{(1)} \rangle) = \partial_y (h \langle Kq \rangle \partial_x \bar{c}) + \partial_y \langle \Phi \rangle \partial_x \bar{c} - \partial_y (h \langle D_1 \rangle \partial_x \bar{c}). \quad (\text{A } 7)$$

Since there is no net flux of contaminant across the shoreline, this equation can be integrated at sight to give the result

$$\partial_y \langle \|c\|^{(1)} \rangle = \left\{ \frac{\langle Kq \rangle}{\langle K \rangle} + \frac{\langle \Phi \rangle}{h \langle K \rangle} - \frac{\langle D_1 \rangle}{\langle K \rangle} \right\} \partial_x \bar{c}. \quad (\text{A } 8)$$

Thus, in the now classical manner of dispersion calculations, the steady and unsteady transverse concentration gradients are both proportional to the longitudinal gradient (Taylor 1953). At this same order in  $\epsilon$ , the unsteady terms in equation (A 3) can be written

$$h \partial_\tau \|c\|^{(2)} = -h \|u\|' \partial_x \|c\|^{(1)} - h \|v\| \partial_y \|c\|^{(1)} - \partial_y \Phi' \partial_x \bar{c} + \partial_y (h K \partial_y \|c\|^{(1)})' + \partial_y (h D_1' \partial_x \bar{c}). \quad (\text{A } 9)$$

Finally, we take cross-sectional and tidal averages of equation (A 3) and, retaining only the dominant (order  $\epsilon^3$ ) terms, we obtain the longitudinal dispersion equation

$$\begin{aligned} A \partial_T \bar{c} + Q \partial_x \bar{c} + \partial_x \int_{y^-}^{y^+} h \langle \|u\|' \|c\|^{(2)} \rangle dy - \partial_x \int_{y^-}^{y^+} \langle \Phi \partial_y \|c\|^{(1)} \rangle dy \\ = \partial_x \int_{y^-}^{y^+} h \langle D_0 \rangle \partial_x \bar{c} dy + \partial_x \int_{y^-}^{y^+} h \langle D_1 \rangle \partial_y \|c\|^{(1)} dy. \end{aligned} \quad (\text{A } 10)$$

Here  $A$  is the local cross-sectional area of the estuary and  $Q$  is the volume discharge rate of fresh water along the estuary. To convert this equation into the standard form we perform one integration by parts with respect to  $\tau$  on the  $h \langle \|u\|' \|c\|^{(2)} \rangle$  term, substitute for  $h \partial_\tau \|c\|^{(2)}$  from equation (A 9), and then perform an integration by parts with respect to  $y$ . In this way we arrive at the equation

$$A \partial_T \bar{c} + Q \partial_x \bar{c} - \partial_x (A E \partial_x \bar{c}) = 0, \quad (\text{A } 11)$$

where the longitudinal dispersion coefficient  $E$  is given by the lengthy expression

$$E = \frac{1}{A} \int_{y_-}^{y_+} \left\{ \langle Kq^2 \rangle - \frac{\langle Kq \rangle^2}{\langle K \rangle} + 2 \frac{\langle Kq \rangle \langle D_1 \rangle}{\langle K \rangle} + \langle D_0 \rangle - 2 \langle D_1 q \rangle - \frac{\langle D_1 \rangle^2}{\langle K \rangle} + \frac{\langle \Phi \rangle^2}{h^2 \langle K \rangle} \right\} h \, dy. \quad (\text{A } 12)$$

Equation (A 12) can be recognized as being equal to the sum  $E_S + E_T + E_V$  of the three dominant contributions to the longitudinal dispersion coefficient (equations (7.15), (7.16), (7.17)). Thus, we have an alternative derivation of the rather complicated key result in the above paper. A great deal more work would be needed to confirm the applicability of equation (A 1) in the present physical context (i.e. unsteady motion in water of non-uniform depth). However, it is reassuring that the results (7.15)–(7.17) can be recovered in their entirety.

#### REFERENCES

- Bowden, K. F. 1965 Horizontal mixing in the sea due to a shearing current. *J. Fluid Mech.* **21**, 83–95.
- Breusers, H. N. C. (ed.) 1974 Momentum and mass transfer in stratified flows. *Delft Hydraul. Lab. Rep.* no. 880.
- Chatwin, P. C. 1971 On the interpretation of some longitudinal dispersion experiments. *J. Fluid Mech.* **48**, 689–702.
- Chatwin, P. C. 1973 A calculation illustrating effects of the viscous sub layer on longitudinal dispersion. *Q. Jl Mech. appl. Math.* **26**, 427–439.
- Chatwin, P. C. 1975 On the longitudinal dispersion of passive contaminant in oscillatory flows in tubes. *J. Fluid Mech.* **71**, 513–527.
- Chatwin, P. C. 1976 Some remarks on the maintenance of the salinity distribution in estuaries. *Estuarine Coastal Mar. Sci.* **4**, 555–566.
- Cole, J. D. 1968 *Perturbation methods in applied mathematics*. Waltham, Mass.: Blaisdell.
- Dyer, K. R. 1978 Lateral circulation effects in estuaries. *N.A.S. Symposium on Geophysics of Estuaries*.
- Elder, J. W. 1959 The dispersion of marked fluid in turbulent shear flow. *J. Fluid Mech.* **5**, 544–560.
- Erdogan, M. E. & Chatwin, P. C. 1967 The effects of curvature and buoyancy on the longitudinal dispersion of solute in a horizontal tube. *J. Fluid Mech.* **29**, 465–484.
- Fischer, H. B. 1967 The mechanics of dispersion in natural streams. *J. Hydraul. Div. A.S.C.E.* **93**, 187–216.
- Fischer, H. B. 1972 Mass transport mechanisms in partially stratified estuaries. *J. Fluid Mech.* **53**, 671–687.
- Fischer, H. B. 1973 Longitudinal dispersion and turbulent mixing in open channel flow. *A. Rev. Fluid Mech.* **5**, 59–78.
- Fischer, H. B. 1976 Mixing and dispersion in estuaries. *A. Rev. Fluid Mech.* **8**, 107–133.
- Hansen, D. V. & Rattray, M. 1965 Gravitational circulation in straits and estuaries. *J. Mar. Res.* **23**, 104–122.
- Holley, E. R., Harleman, D. R. F. & Fischer, H. B. 1970 Dispersion in homogeneous estuary flow. *J. Hydraul. Div. A.S.C.E.* **96**, 1691–1709.
- Imberger, J. 1976 Dynamics of a longitudinally stratified estuary. *Proc. 15th Int. Conf. Coastal Engng., Hawaii*, 3108–3117.
- Le Blond, P. H. 1978 On tidal propagation in shallow rivers. *J. Geophys. Res.* **83**, 4717–4721.
- Macqueen, J. F. 1978a On factors affecting longitudinal mixing in tidal waterways. Central Electricity Research Laboratories no. RD/L/N127/78.
- Macqueen, J. F. 1978b On the far-field temperatures associated with cooling water discharges from estuarine power stations. Central Electricity Research Laboratories no. RD/L/N128/78.
- Macqueen, J. F. 1979 Turbulence and cooling water discharges. *Mathematical modelling of turbulent diffusion in the environment* (ed. C. J. Harris). New York: Academic Press.
- Maxey, M. R. 1978 Aspects of unsteady turbulent shear flow. Ph.D. thesis, University of Cambridge.
- Okubo, A. 1967 The effect of shear in an oscillatory current on horizontal diffusion from an instantaneous source. *Int. J. Oceanol. Limnol.* **1**, 194–204.
- Smith, R. 1976 Longitudinal dispersion of a buoyant contaminant in a shallow channel. *J. Fluid Mech.* **78**, 677–688.
- Smith, R. 1977 Long-term dispersion of contaminants in small estuaries. *J. Fluid Mech.* **82**, 129–146.
- Smith, R. 1978a Coriolis curvature and buoyancy effects upon dispersion in a narrow channel. *Hydraulics of estuaries and fjords* (ed. J. C. J. Nihoul), pp. 217–232. Amsterdam: Elsevier.
- Smith, R. 1978b Asymptotic solutions of the Erdogan–Chatwin equation. *J. Fluid Mech.* **88**, 323–337.
- Smith, R. 1979 Buoyancy effects upon lateral dispersion in open-channel flow. *J. Fluid Mech.* **90**, 761–779.
- Talbot, J. R. & Talbot, G. A. 1974 Diffusion in shallow seas and in English coastal and estuarine waters. *Rapp. P-v. Reun. Cons. Int. Explor. Mer.* **167**, 93–110.

Taylor, G. I. 1953 Dispersion of soluble matter in solvent flowing slowly through a tube. *Proc. R. Soc. Lond.* A **219**, 186–203.

Uncles, R. J. & Radford, P. J. 1980 Seasonal and spring-neap tidal dependence of axial dispersion coefficients in the Severn estuary. *J. Fluid Mech.* (in the press.)

Williams, D. J. A. & West, J. R. 1973 A one-dimensional representation of mixing in the Tay estuary. *Mathematical and hydraulic modelling of estuarine pollution*. London: H.M.S.O.